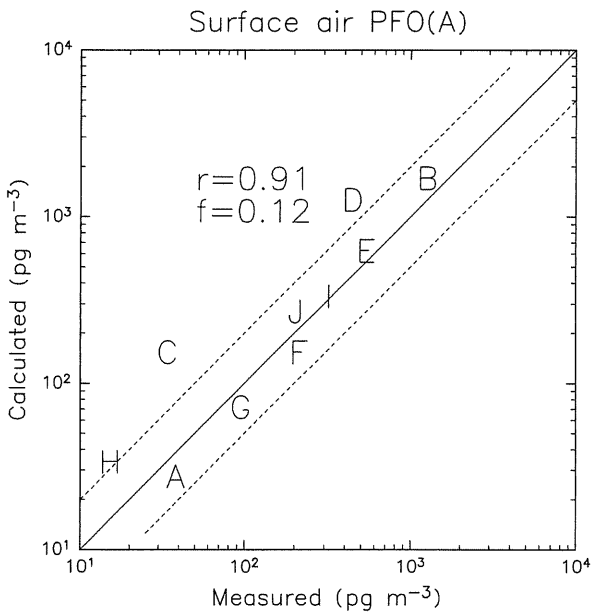

FIGURE 2. Comparison of observed and modeled surface air concentrations in the 2000s (pg m^{-3}) at various sampling sites. Agreement is indicated by a correlation coefficient r of 0.91 (p = 2.6 × 10^{-4}) and an averaged fractional difference f of 0.12. Observations at sampling sites (*6–8*) are denoted A, B, and so on. Geographical locations are given in Table S3. Symbols on the solid line indicate a perfect fit between observation and calculation, and those lying between the two dashed lines indicate error factors of less than 2.

model simulations generally matched observed concentrations in the 2000s as indicated by a high correlation coefficient of 0.91 (p = 2.6 × 10^{-4}) as shown in Figure 2. General agreement was also indicated by an f value of 0.12. Seven out of ten samples were reproduced with an error factor lower than 2. The error factors of the three other samples (C, D, and H) were lower than 5. The presence of error factors higher than 2 may have been due to an inaccuracy of the predicted wind fields or of the topography around the sampling sites. Additional observations are necessary to further evaluate the atmospheric model.

Estimated PFO(A) Intake. Reflecting surface air concentrations, estimated inhaled intake in Settsu was 1 order of magnitude greater than that in Kyoto and Nishinomiya, which was comparable to our previous estimate of 3.9 ng day^{-1} (*6*) (Figure S4). Likewise, the inhaled intake in Osaka was negligible, although it was consistently greater than in Kyoto and Nishinomiya. The inhaled intake in Settsu exceeded 50 ng day^{-1} for most of the period, and it was much greater than the estimated GIT intake until 2005. Spikes in inhaled intake levels resulted from variability in air concentrations.

Serum Levels of PFO(A) in Residents of the Keihanshin Area. Figure 3 shows temporal trends of serum PFO(A) levels on a logarithmic scale for residents of the Settsu area, Kyoto area, Nishinomiya area, and Osaka areas. Inhaled intakes were assumed to be homogeneous for each target population, whereas GIT intakes were variable among individuals in general population. The model results represented variable in GIT intakes by the lower and upper bounds. Figure 3 also compares calculated serum levels with observed levels in the samples collected in these areas (*2, 3, 24, 25*). The model reproduces temporal trends found in the samples in Settsu and Kyoto, where levels increased until 2005 and then decreased. Calculated serum levels generally agreed with observations as indicated by a high correlation coefficient r of 0.93 (p = 9.5 × 10^{-5}) and a small

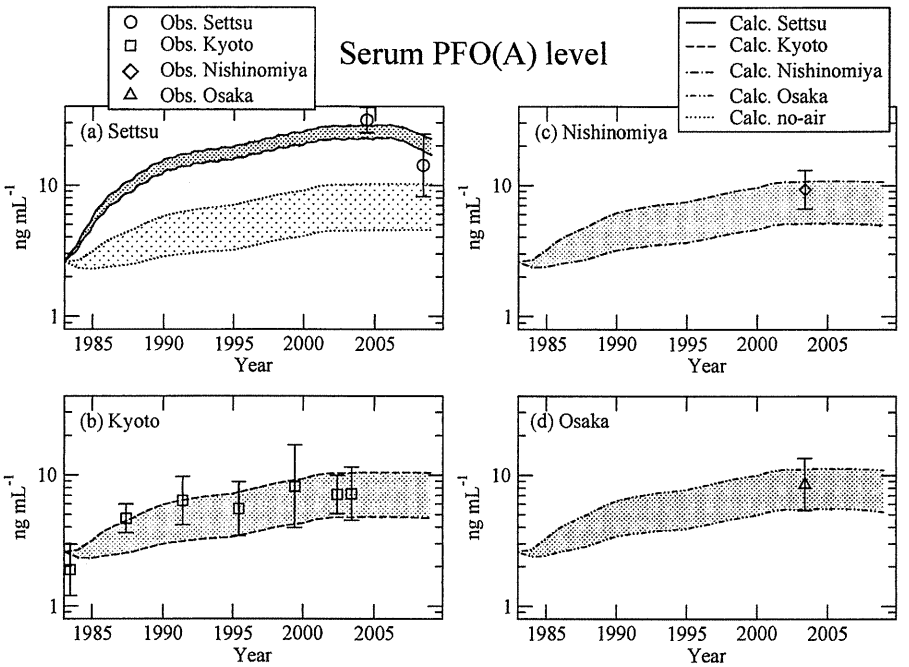

FIGURE 3. Serum PFO(A) levels on a logarithmic scale (lines, in ng mL^{-1}) calculated using simulated surface air concentrations and observed in samples from residents. The model reproduced the temporal trend of serum concentrations of PFO(A) in residents living in the Settsu area (a) and the Kyoto area (b). The modeled levels also agreed with observations in 2003 from the Nishinomiya area (c) and from Osaka residents (d). The case without respiratory exposure (no-air) is also shown (a). The results of the no-air run almost overlapped with those of the control run for Kyoto, Nishinomiya, and Osaka. Symbols represent GM of observed serum PFO(A) levels (*2, 3, 24, 25*) for Settsu (circle), Kyoto (square), Nishinomiya (diamond), and Osaka (triangle). Error bars represent one GSD. Lower and upper bounds of calculated serum values are shown by belts. The values correspond to serum levels for GIT intake at the 25th and 75th percentiles of values extrapolated from observed values in 2004 (*3*).

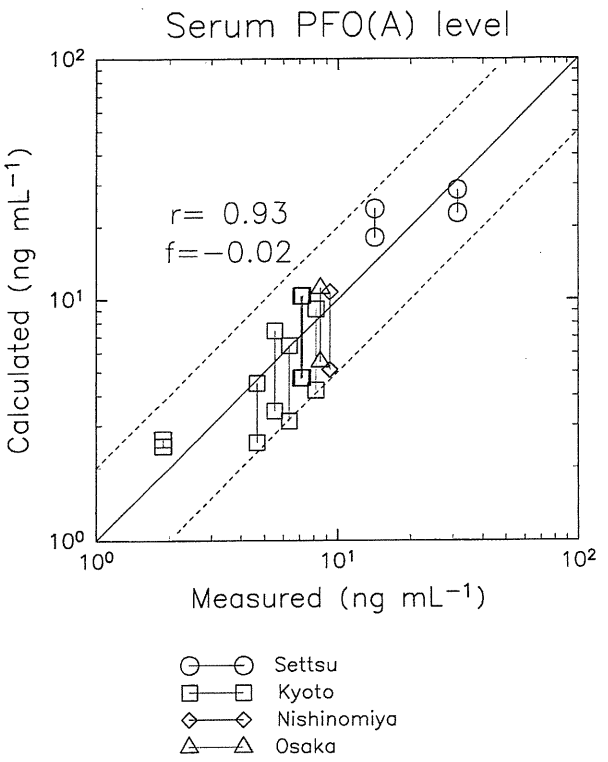

FIGURE 4. Comparison of serum PFO(A) levels (ng mL^{-1}) between model results and observations listed in Table S4 (*2, 3, 24, 25*). Agreement is indicated by a correlation coefficient *r* of 0.93 ($p = 9.6 \times 10^{-5}$) and an averaged fractional difference *f* of −0.02. The calculated concentrations are represented by line segments using the lower and the upper limits of GIT intake (black for Settsu, red for Kyoto, green for Nishinomiya, and blue for Osaka). The observed concentrations are GM from each set of samples. The two dashed lines indicate an error factor of 2; *r* and *f* were calculated using the average of the lower and upper limits of modeled concentrations.

fractional difference *f* of −0.02 (Figure 4). All eleven samples were reproduced by error factors less than 2.

Serum levels for the case without inhaled intake (no-air run) are also shown in Figure 3. Differences between the control run and the no-air run represent the atmospheric PFO(A) contribution to total serum levels. The atmospheric contributions are dominant in Settsu (from 67.4% in the upper oral intake case to 79.8% in the lower oral intake case in 2008) but negligible in Kyoto and Nishinomiya. Modeled PFO(A) levels for Osaka residents are similar to those of the Kyoto area and Nishinomiya area. The model results reveal that the high PFO(A) level of 31.4 ng mL^{-1} observed in Settsu in 2004 is attributed mainly to the atmospheric component. It should be noted that serum concentration levels of PFO(A) in the Keihanshin area are greater than those in other areas (*2, 3*). Excess PFO(A) intake by residents of the Keihanshin area may be attributed to their consumption of drinking water (*4*). However, specifying contributions of various sources of intake requires further study.

The serum levels of Settsu residents decreased after 2005 as a result of emission control by the manufacturer. However, PFO(A) levels in Keihanshin residents remained higher than levels in other areas, which were less than 5 ng mL^{-1} in the 2000s (*2, 3*). The persistence of PFO(A) is attributed to its long half-life.

Recent epidemiological studies have suggested that PFO(A) may have adverse health effects on fetal growth at much lower serum concentrations in mothers (*27, 28*) than those observed in females of Settsu in 2008. For this reason, adverse health effects on fetal and neonatal growth should be evaluated epidemiologically in the population within a 4.5 km radius of the Daikin plant.

In this study, we combined an atmospheric model and a PK model to evaluate long-term inhalation exposure to PFO(A) in the Osaka urban area. The model results for PFO(A) concentrations both in surface air and in human serum generally agree with observations. Sensitivity analysis demonstrated that changes in model parameters did not have profound effects on the simulation results [Supporting Information (section S6)]. However, it is necessary to characterize chemical and physical properties in the atmosphere as well as the pharmacokinetic behavior of PFO(A) in greater detail. For example, particle size and absorption by the respiratory tract are not fully understood.

It should be noted that the target domain in this study is small and near a strong point source. Other sources are assumed to be negligible. For large-scale modeling, other sources should be included such as gaseous PFOA emission by volatilization from the surface of the earth (*29*) and by release from marine aerosols enriched with surfactant PFO (*30*). It should be also noted that there is an argument regarding the irreversibility of gaseous PFOA sorption by QFFs (*31, 32*). To observe the atmospheric PFO(A) more accurately, it might be necessary that PFO(A) on particulate matter and gaseous PFOA are collected separately and simultaneously by appropriate devices, such as surface-deactivated QFFs and downstream sorbents (*12*).

The combination of atmospheric transport modeling and PK modeling has great potential. When modeling results are validated by comparisons with monitoring samples from human specimen banks, they can aid in reconstruction of human exposure intensity over previous decades. This approach can be applied to other chemicals and to other regions where both human blood and food duplicate samples are available. In an earlier study, we developed a global atmospheric transport model for long-term simulation of atmospheric lead (*33*). Using the approach described herein, we are now expanding that work to the study of human exposure to atmospheric lead from 1979 to 2009 in four East Asian countries: Japan, Korea, China, and Vietnam.

Here, we have demonstrated an approach to reconstruction of historical human exposure using existing estimates of emissions. Atmospheric modeling in combination with PK modeling can also serve to assess unknown emissions or to predict human exposure trends in the future using various emission scenarios. Therefore, this approach will be useful not only in emission control but also in environmental decision making.

Acknowledgments

This project was supported primarily by the Japan Science and Technology Agency (1300001, 2008–2010). The meteorological data used in this study were from the JRA-25 long-term reanalysis data set developed in a cooperative research project of the Japan Meteorological Agency and the Central Research Institute of Electric Power Industry.

Supporting Information Available

Information regarding model options and modifications as well as additional results and discussion. This material is available free of charge via the Internet at http://pubs.acs.org.

Literature Cited

(1) *The Science Advisory Board (SAB) review of EPA's draft risk assessment of potential human health effects associated with PFOA and its salts*; EPA-SAB-06-006; U.S. Environmental Protection Agency: Washington, DC, 2006. www.epa.gov/sab/pdf/sab_06_006.pdf (accessed January 10, 2010).

(2) Harada, K.; Koizumi, A.; Saito, N.; Inoue, K.; Yoshinaga, T.; Date, C.; Fujii, S.; Hachiya, N.; Hirosawa, I.; Koda, S.; Kusaka, Y.; Murata, K.; Omae, K.; Shimbo, S.; Takenaka, K.; Takeshita,

T.; Todoriki, H.; Wata, Y.; Watanabe, T.; Ikeda, M. Historical and geographical aspects of the increasing perfluorooctanoate and perfluorooctane sulfonate contamination in human serum in Japan. *Chemosphere* **2007**, *66*, 293–301, DOI 10.1016/j.chemosphere.2006.05.010.

(3) Kärrman, A.; Harada, K.; Inoue, K.; Takasuga, T.; Ohi, E.; Koizumi, A. Relationship between dietary exposure and serum perfluorochemical (PFC) levels—A case study. *Environ. Int.* **2009**, *35*, 712–717, DOI 10.1016/j.envint.2009.01.010.

(4) Saito, N.; Harada, K.; Inoue, K.; Sasaki, K.; Yoshinaga, T.; Koizumi, A. Perfluorooctanoate and perfluorooctane sulfonate concentrations in surface water in Japan. *J. Occup. Health* **2004**, *46*, 49–59.

(5) Morikawa, A.; Kamei, N.; Harada, K.; Inoue, K.; Yoshinaga, T.; Saito, N.; Koizumi, A. The bioconcentration factor of perfluorooctane sulfonate is significantly larger than that of perfluorooctanoate in wild turtles (*Trachemys scripta elegans* and *Chinemys reevesii*): An Ai river ecological study in Japan. *Ecotoxicol. Environ. Saf.* **2006**, *65*, 14–21, DOI 10.1016/j.ecoenv.2005.03.007.

(6) Harada, K.; Nakanishi, S.; Sasaki, K.; Furuyama, K.; Nakayama, S.; Saito, N.; Yamakawa, K.; Koizumi, A. Particle size distribution and respiratory deposition estimates of airborne perfluorooctanoate and perfluorooctanosulfonate in Kyoto area, Japan. *Bull. Environ. Contam. Toxicol.* **2006**, *76*, 306–310, DOI 10.1007/s00128-006-0922-1.

(7) Harada, K.; Nakanishi, S.; Saito, N.; Tsutsui, T.; Koizumi, A. Airborne perfluorooctanoate may be a substantial source contamination in Kyoto area, Japan. *Bull. Environ. Contam. Toxicol.* **2005**, *74*, 64–69.

(8) *Chemicals in the environment: Report on environmental survey and monitoring of chemicals in FY2005*; Environmental Health Department, Ministry of the Environment, Ministry of Japan: Tokyo, 2005 www.env.go.jp/chemi/kurohon/en/http2005e/03-cie/cie2005.pdf (accessed January 10, 2010).

(9) Grell, G. A.; Peckham, S. E.; Schmitz, R.; McKeen, S. A.; Frost, G.; Skamarock, W. C.; Eder, B. Fully coupled "online" chemistry within the WRF model. *Atmos. Environ.* **2005**, *39*, 6957–6975, DOI 10.1016/j.atmosenv.2005.04.027.

(10) Skamarock, W. C.; Klemp, J. B.; Klemp, J. B.; Dudhia, J.; Gill, D. O.; Barker, D. M.; Duda, M. G.; Huang, X.-Y.; Wang, W.; Powers, J. G. A description of the Advanced Research WRF Version 3. *NCAR Tech. Note* 2008NCAR/TN-475+STR.

(11) Onogi, K.; Tsutsui, J.; Koide, H.; Sakamoto, M.; Kobayashi, S.; Hatsushika, H.; Matsumoto, T.; Yamazaki, N.; Kamahori, H.; Takahashi, K.; Kadokura, S.; Wada, K.; Kato, K.; Oyama, R.; Ose, T.; Mannoji, N.; Taira, R. The JRA-25 reanalysis. *J. Meteorol. Soc. Jpn.* **2007**, *85*, 369–432.

(12) Arp, H. P. H.; Goss, K.-U. Irreversible sorption of trace concentrations of perfluorocarboxylic acids to fiber filters used for air sampling. *Atmos. Environ.* **2008**, *42*, 6869–6872, DOI 10.1016/j.atmosenv.2008.05.012.

(13) Prevedouros, K.; Cousins, I. T.; Buck, R. C.; Korzeniowski, S. H. Source, fate and transport of perfluorocarboxylates. *Environ. Sci. Technol.* **2006**, *40*, 32–44, DOI 10.1021/es0512475.

(14) *The supply and demand trend of material fluoropolymer* (in Japanese). www.jfia.gr.jp/jfiadata/jyukyu.htm (accessed January 10, 2010).

(15) *PFOA abolition in fluorochemicals* (in Japanese). www.daikin.co.jp/press/2007/071221/press_20071221.pdf (accessed January 10, 2010).

(16) Wallington, T. J.; Hurley, M. D.; Xia, J.; Wuebbles, D. J.; Sillman, S.; Ito, A.; Penner, J. E.; Ellis, D. A.; Martin, J.; Mabury, S. A.; Nielsen, O. J.; Sulbaek Andersen, M. P. Formation of $C_7F_{15}COOH$ (PFOA) and other perfluorocarboxylic acids during the atmospheric oxidation of 8:2 fluorotelomer alcohol. *Environ. Sci. Technol.* **2006**, *40*, 924–930.

(17) Harada, K.; Inoue, K.; Morikawa, A.; Yoshinaga, T.; Saito, N.; Koizumi, A. Renal clearance of perfluorooctane sulfonate and perfluorooctanoate in humans and their species-specific excretion. *Environ. Res.* **2005**, *99*, 253–261, DOI 10.1016/j.envres.2004.12.003.

(18) Olsen, G. W.; Burris, J. M.; Ehresman, D. J.; Froehlich, J. W.; Seacat, A. M.; Butenhoff, J. L.; Zobel, L. R. Half-life of serum elimination of perfluorooctanesulfonate, perfluorohexanesulfonate, and perfluorooctanoate in retired fluorochemical production workers. *Environ. Health Perspect.* **2007**, *115*, 1298–1305.

(19) Hallberg, L.; Hoddahl, A. M.; Nilsson, L.; Rybo, G. Menstrual blood loss—a population study: variation at different ages and attempts to define normality. *Acta Obstet. Gynecol. Scand.* **1966**, *45*, 320–351.

(20) Vestergren, R.; Cousins, I. T. Tracking the pathways of human exposure to perfluorocarboxylates. *Environ. Sci. Technol.* **2009**, *43*, 5565–5575, DOI 10.1021/es900228k.

(21) Harada, K. H.; Hashida, S.; Kaneko, T.; Takenaka, K.; Minata, M.; Inoue, K.; Saito, N.; Koizumi, A. Biliary excretion and cerebrospinal fluid partition of perfluorooctanoate and perfluorooctane sulfonate in humans. *Environ. Toxicol. Pharmacol.* **2007**, *24*, 134–139, DOI 10.1016/j.etap.2007.04.003.

(22) *Report of the Task Group on Reference Man: a report/prepared by a task group of Committee 2 of the International Commission on Radiological Protection*; ICRP publication No. 23; Pergamon Press: Oxford, New York, 1975.

(23) Koizumi, A.; Harada, K.; Inoue, K.; Hitomi, T.; Yang, H.-R.; Moon, C.-S.; Wang, P.; Hung, N. N.; Watanabe, T.; Shimbo, S.; Ikeda, M. Past, present, and future of environmental specimen banks. *Environ. Health Prev. Med.* **2009**, *14*, 307–318, DOI 10.1007/s12199-009-0101-1.

(24) Harada, K.; Saito, N.; Inoue, K.; Yoshinaga, T.; Watanabe, T.; Sasaki, S.; Kamiyama, S.; Koizumi, A. The influence of time, sex and geographic factors on levels of perfluorooctane sulfonate and perfluorooctanoate in human serum over the last 25 years. *J. Occup. Health* **2004**, *46*, 141–147.

(25) Harada, K. H.; Yang, H.-R.; Moon, C.-S.; Hung, N. N.; Hitomi, T.; Inoue, K.; Niisoe, T.; Watanabe, T.; Kamiyama, S.; Takenaka, K.; Kim, M.-Y.; Watanabe, K.; Takasuga, T.; Koizumi, A. Levels of perfluorooctane sulfonate and perfluorooctanoic acid in female serum samples from Japan in 2008, Korea in 1994–2008 and Vietnam in 2007–2008. *Chemosphere* **2010**, *79*, 314–319, DOI 10.1016/j.chemosphere.2010.01.027.

(26) Kasibhatla, P.; Chameides, W. L.; St. John, J. A three-dimensional global model investigation of seasonal variations in the atmospheric burden of anthropogenic sulfate aerosols. *J. Geophys. Res.* **1997**, *102*, 3737–3760.

(27) Fei, C.; McLaughlin, J. K.; Lipworth, L.; Olsen, J. Maternal levels of perfluorinated chemicals and subfecundity. *Hum. Reprod.* **2009**, *24*, 1200–1205, DOI 10.1093/humrep/den490.

(28) Washino, N.; Saijo, Y.; Sasaki, S.; Kato, S.; Ban, S.; Konishi, K.; Ito, R.; Nakata, A.; Iwasaki, Y.; Saito, K.; Nakazawa, H.; Kishi, R. Correlations between prenatal exposure to perfluorinated chemicals and reduced fetal growth. *Environ. Health Perspect.* **2009**, *117*, 660–667.

(29) Kim, S.-K.; Kannan, K. Perfluorinated acids in air, rain, snow, surface runoff, and lakes: Relative importance of pathways to contamination of urban lakes. *Environ. Sci. Technol.* **2007**, *41*, 8328–8334, DOI 10.1021/es072107t.

(30) Mcmurdo, C. J.; Ellis, D. A.; Webster, E.; Butler, J.; Christensen, R. D.; Reid, L. K. Aerosol enrichment of the surfactant PFO and mediation of the water—air transport of gaseous PFOA. *Environ. Sci. Technol.* **2008**, *42*, 3969–3974.

(31) Barton, C. A.; Kaiser, M. A.; Butler, L. E.; Botelho, M. A. Comment on "Irreversible sorption of trace concentrations of perfluorocarboxylic acids to fiber filters used for air sampling" by Arp and Goss (Atmospheric Environment 42, 6869–6872, 2008). *Atmos. Environ.* **2009**, *43*, 3652–3653.

(32) Arp, H. P. H.; Goss, K.-U. Response to Comment on "Irreversible sorption of trace concentrations of perfluorocarboxylic acid to fiber filters used for air sampling" by Arp and Goss (Atmospheric Environment 42, 6869–6872, 2008). *Atmos. Environ.* **2009**, *43*, 3654–3655.

(33) Niisoe, T.; Nakamura, E.; Harada, K.; Ishikawa, H.; Hitomi, T.; Watanabe, T.; Wang, Z.; Koizumi, A. A global transport model of lead in the atmosphere. *Atmos. Environ.* **2010**, *44*, 1806–1814, DOI 10.1016/j.atmosenv.2010.01.001.

ES101948B

Atmospheric Environment 44 (2010) 1806–1814

Contents lists available at ScienceDirect

Atmospheric Environment

journal homepage: www.elsevier.com/locate/atmosenv

A global transport model of lead in the atmosphere

T. Niisoe [a], E. Nakamura [a], K. Harada [a], H. Ishikawa [b], T. Hitomi [a], T. Watanabe [c], Z. Wang [d], A. Koizumi [a,*]

[a] Department of Health and Environmental Sciences, Graduate School of Medicine, Kyoto University, Kyoto 606-8501, Japan
[b] Research Division of Atmospheric and Hydrospheric Disasters, Disaster Prevention Research Institute, Kyoto University, Uji 611-0011, Japan
[c] Miyagi University of Education, Miyagi 980-0845, Japan
[d] Institute of Atmospheric Physics, Chinese Academy of Sciences, Beijing 100029, China

ARTICLE INFO

Article history:
Received 25 March 2009
Received in revised form
6 January 2010
Accepted 7 January 2010

Keywords:
Transport model
Atmospheric lead
Heavy metal
Particulate matter

ABSTRACT

A global atmospheric transport model is used to calculate lead concentrations in the atmosphere. The model performance is evaluated through comparisons with observations in Europe. The model results of lead concentrations in surface air were compared with measurements in East Asia. The detailed comparisons showed generally good agreement for recent decades, although systematic underestimation was found in China. Anthropogenic lead emissions in China are estimated from economic statistics to be 56 000 t yr^{-1}, which is not small considering the economic scale of China. The underestimations suggest a hidden source of lead emissions. The emissions in Japan and Korea are derived from optimization by the model. The magnitude is about 2000 t yr^{-1}, which is much greater than that reported by the Pollutant Release and Transfer Register in Japan and Toxics Release Inventory in Korea.

1. Introduction

Lead is one of the most abundant hazardous heavy metals in the atmosphere. It exists in particulate matter in the atmosphere and is transported to a large extent by air flow. Lead enters the human body through inhalation and the consumption of food and water, and this could have serious adverse effects on human health. Leaded gasoline is recognized as being the largest source of atmospheric lead followed by nonferrous metal production and fossil fuel combustion.

In many developed countries, anthropogenic lead emission has been reduced remarkably in recent years because of the phasing out of leaded gasoline and industrial emission controls (e.g. Ilyin et al., 2007a). On the other hand, efforts to reduce emissions are insufficient in many Asian countries, several of which are in rapid economic progress. Although it is urgent to establish a system to assess transboundary air pollutants in Asia, a monitoring network and infrastructure for sharing information have not yet been established and are not likely to be established in the near future. Therefore, the development of a numerical modeling framework as a common and cost-conscious tool is required to assess atmospheric pollutants in Asia.

In this work, a global atmospheric transport model is presented to estimate long-term air concentrations and depositions of lead from the 1980s to 2000s. This project is a first step in establishing an assessment system for transboundary air pollutants in East Asia. The transport model used in this study is not unique, but we formalized all necessary processes. The model has advantage for numerical cost using an existing meteorological field. We also collected information and parameters for atmospheric lead assessment in Asian countries. We conducted a detailed and comprehensive comparison between results of a long-term model simulation and observations in East Asia of the atmospheric concentration.

2. Materials and methods

The numerical models and datasets used for model validation in the present study are described in this section. Tables and figures with numbering preceded by S are given in Section 3 of the Supplementary material.

2.1. Experiment methodology

An atmospheric transport model of lead was developed, and numerical simulations were carried out from 1979 to 2007. To evaluate the model performance, the model predictions were compared with observations in Europe, where information on lead emissions has high reliability and long-term observations are available. Lead concentrations in the atmosphere predicted by the model were then compared with observations in East Asia. The observed concentrations in Japan and Korea were compared with the model results. The model was run for two different emission

* Corresponding author. Tel.: +81 75 753 4456; fax: +81 75 753 4458.
E-mail address: Akio.Koizumi@z06.mbox.media.kyoto-u.ac.jp (A. Koizumi).

1352-2310/$ – see front matter © 2010 Elsevier Ltd. All rights reserved.
doi:10.1016/j.atmosenv.2010.01.001

data sources in Japan and Korea; one dataset was derived from the national inventories and the other from an optimization of a pre-existing grid data.

2.2. Atmospheric transport model

Atmospheric lead is emitted in the form of fine particle mainly directly from leaded gasoline use, nonferrous metal production and fossil fuel combustion. Lead has no significant chemical process in the atmosphere. The removal of atmospheric lead is mediated by dry and wet deposition. It is broadly accepted that the observed mass size distribution of atmospheric lead is typically centered in the 'accumulation mode', corresponding to a diameter of 0.1–1.0 μm (e.g. Allen et al., 2001). The dry deposition velocity depends on the particle size in general, but size dependency is almost negligible for particles with diameters ranging between 0.05 and 2.0 μm (e.g. Slinn et al., 1978). Wet deposition depends on the precipitation rate rather than the particle size. Therefore, we can discard the effects of the size distribution of particles in both dry and wet deposition as is done in preexisting models of atmospheric lead (Ilyin et al., 2007b). We fix the particle size at 1.0 μm.

The numerical model employed in this work is a Eulerian atmospheric transport model. The time evolution of the lead concentration in each grid box is calculated by solving the continuity equation:

$$\frac{\partial c}{\partial t} = -\nabla \cdot \boldsymbol{F}_{\mathrm{trans}} + F_{\mathrm{em}} - F_{\mathrm{dep}},$$

where c is the concentration, F_{trans} is the three-dimensional transport flux, and F_{em} and F_{dep} are the local emission and deposition fluxes. The computation region is the globe and the horizontal resolution is 1.25°. The vertical structure consists of 12 layers with sigma coordinates of 0.99, 0.98, 0.95, 0.92, 0.83, 0.66, 0.55, 0.44, 0.33, 0.22, 0.11 and 0 stacked from the surface to 100 hPa. The typical depth of the lowest layer is about 150 m. The transport and deposition fluxes are assessed using 6-hourly meteorological fields determined from the JRA-25 reanalysis datasets provided by the Japan Meteorological Agency and Central Research Institute of Electric Power Industry (Onogi et al., 2007). The variables used in the model are listed in Table S1. The vertical air velocity in sigma coordinates is converted from the original isopressure coordinates. The change in the concentration is assessed by operator splitting with a time step of 1 h.

Mass-conservative transport flux within the Euler forward time step of 10 min is calculated using a parabolic-spline method (Emde, 1992) for advection and a box method (Kurihara and Holloway, 1967) for diffusion. The horizontal diffusion coefficient is proportional to the magnitude of the derivative of the horizontal wind velocity component parallel to the interface between two adjacent boxes (Mahlman and Moxim, 1978; Levy et al., 1982), and the vertical coefficient depends on the height, shear, and stability (Louis, 1979). The boundary layer height is derived by bulk formulation (Vogelezang and Holtslag, 1996) and the concentration is assumed to be vertically uniform in the boundary layer.

To validate the performance of the transport model, a cone-shaped distribution was advected in rotational wind fields (Williamson and Rasch, 1989). It was confirmed that the model is positive definite, shape preservative and mass conservative with high accuracy even for cross polar advection, and that numerical diffusion is sufficiently small.

Wet deposition modeling includes in-cloud and subcloud scavenging. In-cloud scavenging can occur only in the fraction of a grid box occupied by liquid cloud with precipitation, and subcloud scavenging only in the fraction covered by cloud with precipitation. Vertical transport flux in deep convective clouds is also parameterized by the water–vapor mass balance (Feichter and Crutzen, 1990).

Dry deposition in the lowest layer is estimated using a conventional framework for the dry deposition velocity. The velocity is a function of aerodynamic resistance depending on atmospheric stability and surface roughness, quasi-laminar sublayer resistance depending on the Brownian diffusivity of the particles, and the particle settling velocity given by Stokes' Law (Seinfeld and Pandis, 1998).

The model was run from 1979 to 2007. The initial lead concentration was determined by a preparatory one year run for 1979 starting with zero concentration. The detailed model formulations are described in Section 2.1 of the Supplementary material.

2.3. Lead emission

In this study, two lead sources, one anthropogenic and the other being the sea surface, are considered. Lead is emitted to the lowest layer and is assumed to be uniform inside each grid box. The anthropogenic emissions are assumed to have no seasonal variability.

2.3.1. Anthropogenic emission

The global emission of anthropogenic lead is considered. Different emission datasets are used for Europe, China, Japan and Korea, and the rest of the world.

Global anthropogenic emissions except those for Europe, Japan, Korea, and China are taken from version 1.0 of the global inventory of the Canadian Global Emission Interpretation Centre (CGEIC) (Pacyna et al., 1995). Data are presented in a 1-degree grid system for the reference year 1989. The inventory has a minimum scenario and maximum scenario. The average of the two scenarios is adopted in this work.

For Europe, an anthropogenic lead emission inventory is provided by the European Monitoring and Evaluation Programme (EMEP, http://www.emep.int/). The dataset includes a horizontal distribution of lead emission with 0.5-degree resolution for 1990. For the following years (1991–2007), the dataset gives the annual emission for each country but not the distribution (Tables S2 and S3). Therefore, we assume that the horizontal distributions for 1991 and 2007 are the same as that in 1990 and allocate the annual country emission to the corresponding horizontal grids. There are also missing data, which are replaced by linear interpolation (or extrapolation) in time. The emissions for countries reported only in 1990, which are 6% of the total emission for Europe in 2005, are assumed to be constant. The spatial distribution of lead emissions in 1990 and the temporal variability are shown in Fig. 1. Emissions in Germany and northern Europe are more than 75% less by 1995, and the same is seen for most of Europe by 2005. Emissions before 1990 in Europe are fixed at the European component of the CGEIC inventory.

For China, lead emission is derived from economic statistics for 2001. Annual emission from each province is estimated as fuel consumption and industrial production (Table S4) multiplied by corresponding emission factors (Table S5). Table S6 presents the estimated emission for each province. The total emission for China is 56 000 t yr^{-1}. The total lead emission is horizontally distributed on the basis of three assumptions (Fig. 2): (1) 60% of the total lead emission in each province is allocated to the city with the largest population and cities with populations of more than two million as listed in Table S7, (2) the ratio of emissions from the cities is proportional to the ratio of populations of the cities, and (3) the spatial distribution of the remaining (40%) total emission within each province is the same as that described by the CGEIC emission data.

In Japan and Korea, direct emission inventories are available. The Pollutant Release and Transfer Register (PRTR, http://www.env.go.jp/en/chemi/prtr/prtr.html) has data beginning in 2001 for Japan and the Toxics Release Inventory (TRI, http://tri.nier.go.kr/) has data beginning in 2002 for Korea. Table S8 presents national emissions for Japan and Korea reported by the inventories. The reported

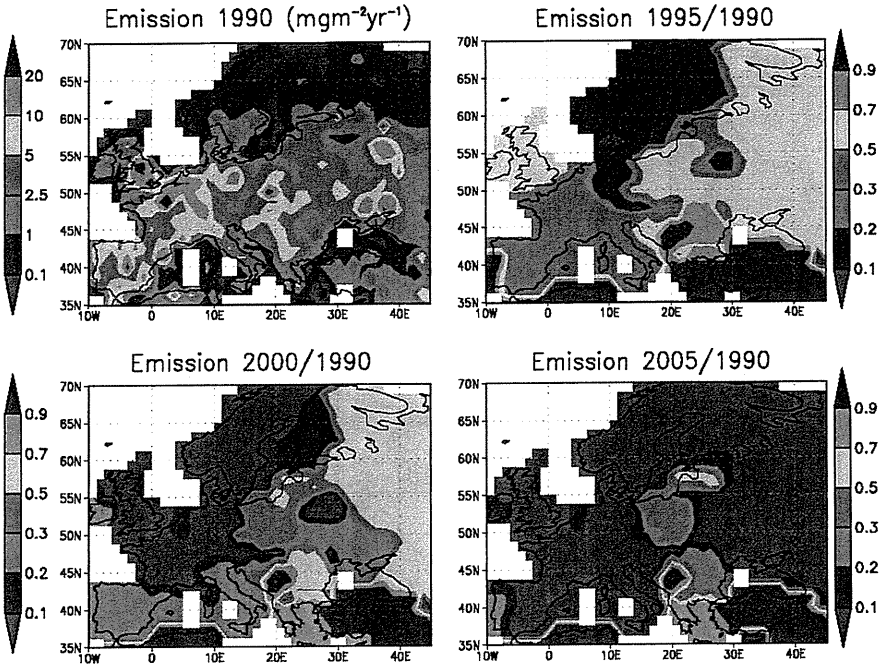

Fig. 1. Reported lead emission flux distributed to the model grid (mg m^{-2} yr^{-1}) for Europe in 1990, and the proportions of emissions in 1995, 2000, and 2005 to the emission in 1990. The yearly lead emissions are reported by the EMEP. Anthropogenic lead emission for most of Europe had decreased significantly during the 1990s.

emissions for Japan and Korea are generally less than those for industrialized countries in Europe during the 2000s, as shown in Table S3. Two datasets of lead emission from Japan and Korea are used for the model. One is made directly from the inventories of the PRTR and TRI. The other is emission data optimized by applying correction factors to the Japanese and Korean components of the CGEIC emission data on the assumption that the distribution inside each nation has not changed from that described by the CGEIC data (Fig. 3).

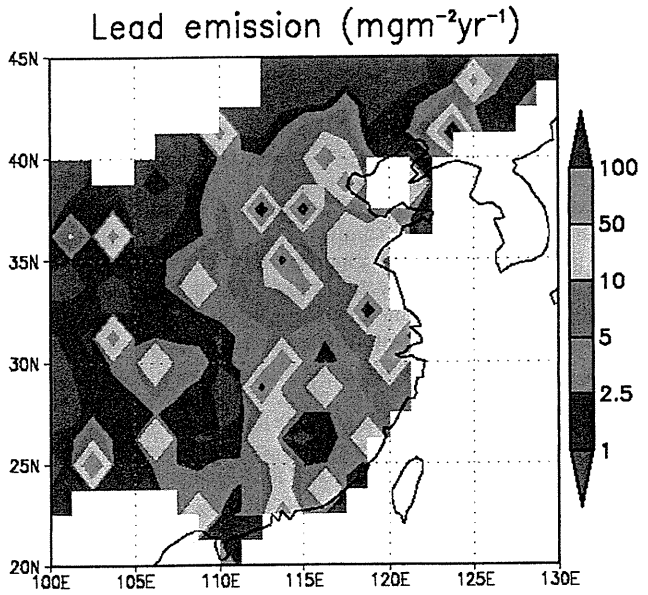

Fig. 2. Lead emission flux distributed to the model grid (mg m^{-2} yr^{-1}) in China estimated as fuel consumption and industrial production multiplied by corresponding emission factors for 2001.

2.3.2. Lead from sea salt

Lead emission from sea salt is derived using an empirical function of the surface wind speed, following the works of Gong (2003) and Ilyin et al. (2007b). The total emission from sea salt is 28 000 t yr^{-1} for 1990. The formulation is described in Section 2.1.7 of the Supplementary material. The emission factor of 4.0 mg kg^{-1}, which has been estimated for the North Atlantic, is used for lead emission from sea water (Ilyin et al., 2007b). Ilyin et al. (2007b) noted that the contribution from the re-suspension of anthropogenic lead historically accumulated in the ocean is not negligible, although it can be overestimated in remote regions.

2.4. Observation datasets

To evaluate the model performance, comparisons with observations are made. In Europe, an atmospheric monitoring network for transboundary air pollutant was established in the late 1980s by the EMEP (Ilyin et al., 2007a). All data from the monitoring stations are binned according to the model resolution into 40 grid boxes for atmospheric lead concentrations and 75 grid boxes for precipitation lead concentrations (Fig. S1). The observed concentrations are averaged inside each box.

In Japan, aerosol particles were collected and analyzed mainly in urban areas by the National Air Surveillance Network from 1974 to 1996 (Var et al., 2000). The measurements have been continued by several local governments. In Korea, a number of heavy-metal monitoring stations in 13 cities throughout the Korean peninsula have been operated by the administrative demand of the Korean Ministry of Environment since 1991 (Kim, 2007). In China, unfortunately, no monitoring network has yet been developed. Therefore, calculated concentrations for China are compared with published observation results listed in Table S9. Observations affected by particular emission sources or meteorological events are excluded as much as possible. As for Europe, the data from the monitoring stations are binned into 23 boxes in Japan, 7 boxes in

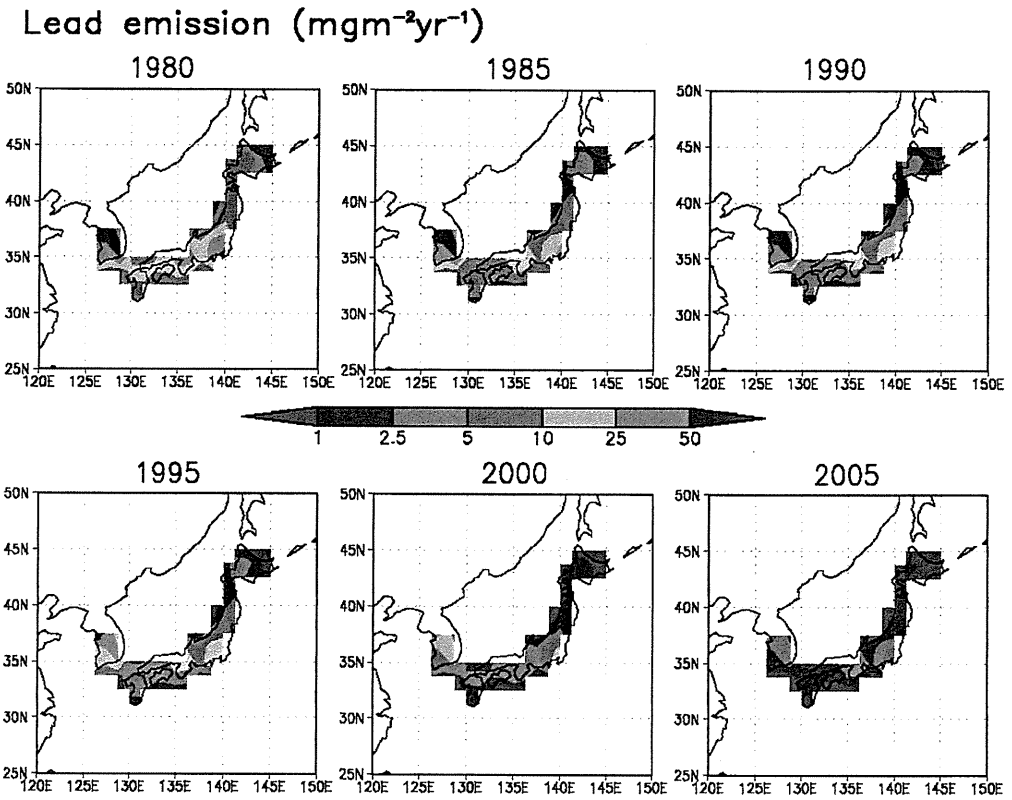

Fig. 3. Estimated lead emission flux distributed to the model grid (mg m^{-2} yr^{-1}) for Japan and Korea from 1980 to 2005. The magnitudes are optimized by applying correction factors to the Japanese and Korean components of the CGEIC emission data.

Korea, and 32 boxes in China (Fig. S2). The average concentrations in Japan are listed in Tables S10–S12.

3. Results

3.1. Model validation using data for the European environment

The calculated concentrations both in air and in precipitation are compared with observations. The discrepancy between the model and observation is indicated by the fractional difference f (Kasibhatla et al., 1997) averaged for all compared grid points:

$$f = \frac{V_{mdl} - V_{obs}}{V_{mdl} + V_{obs}},$$

where V_{mdl} and V_{obs} are the model value and observation value respectively. $|f| < 0.33$ indicates an error factor of less than 2.

Calculated air concentrations generally agree well with measurements for the early 1990s as indicated by $|f|$ values less than 0.33 (Fig. 4). There is slight underestimation in the late 1990s, and this increases in the 2000s. There is a similar tendency for the calculated lead concentrations in rainwater (Fig. 5). Ilyin et al. (2007a) estimated re-suspension lead flux from soil and suggested that it contributed more than 50% of the total emission for Europe in the 2000s, when anthropogenic emission had decreased significantly. The underestimation of atmospheric lead for the 2000s in our simulation is in agreement with the source estimation conducted by Ilyin et al. (2007a). This suggests the existence of other unknown sources of lead. The re-suspension flux can is a strong candidate for an unknown source, as suggested by Ilyin et al. (2007a).

3.2. Lead levels in East Asia

Fig. 6 compares the calculations and observations for China from the 1980s to 2000s. Most of the observed concentrations exceed 100 ng m^{-3}, which is much greater than concentrations observed in Europe. There is no remarkable temporal variability throughout the periods. The model roughly reproduces observed concentrations with an error factor of less than two, although there is general underestimation especially for the 1980s and 1990s.

The surface concentrations observed for Japan and Korea in 2004 are compared with concentrations calculated by the model using the inventories of PRTR for Japan and TRI for Korea. To assess the transboundary contribution, an additional simulation with only the national emission was conducted, and the result is also plotted in Fig. 7. The model results excluding remote sources are an order of magnitude less than observation values. Taking the remote sources into account, there remains an underestimation by a factor of more than two, especially in eastern Japan. The underestimation of the model is attributed not only to the inflow but also to the national emission of lead, although the effect of the inflow is significant. Therefore, it is concluded that both the PRTR and TRI underestimate lead emission, which implies the necessity to use the optimized emissions determined for Japan and Korea instead of the inventories. The results presented hereafter are only those of the model using the optimized emissions.

Fig. 8 shows national lead emissions for Japan, Korea and China in the model from 1979 to 2007. The emissions for Japan and Korea are optimized using the correction factors listed in Table S13, and the emission for China is estimated using economic statistics as described in Section 2.3.1. Japan and Korea have nearly the same

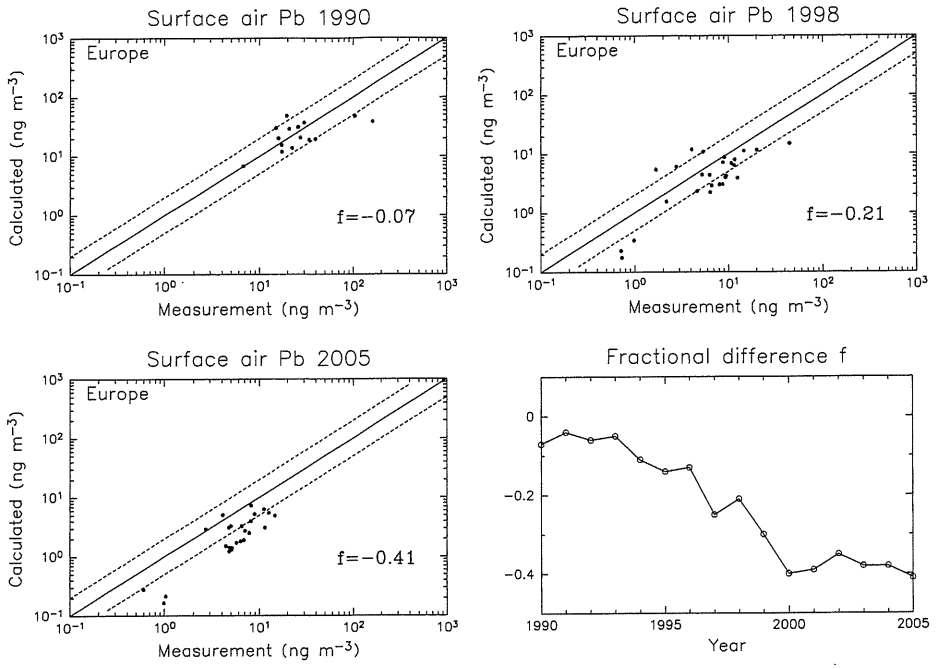

Fig. 4. Scatter plot of annually averaged lead concentrations (ng m^{-3}) at the surface over Europe for the model results and observations in 1990, 1998, and 2005. Dots on the solid line represent a perfect fit between calculation results and observations, and dots between the two dashed lines represent error factors of less than 2. The *f* value is the fractional difference averaged for all pairs of the model results and observations. A time series of the *f* value for each year from 1990 to 2005 is also shown. Generally good agreement in the early 1990s and underestimation in 2000s are demonstrated by descending trend of the *f* value.

magnitude of lead emission, which decreases in the early 1980s and the late 1990s in Japan, and in the early 1990s in Korea. Both Japan and Korea have lead emissions of about 2000 t yr^{-1} in the mid-2000s, which is about 14% of that for 1980. The emission of 56 000 t yr^{-1} for China is much greater than emissions for Japan and Korea. The emissions for Japan, Korea and China are 87% of the total emission for East Asia (100–150E, 0–60N) in 2005.

Comparisons of the calculations and observations of surface lead concentrations for Japan from the 1980s to 2000s show fairly good agreement as indicated by $|f|$ values less than 0.1 for most of the

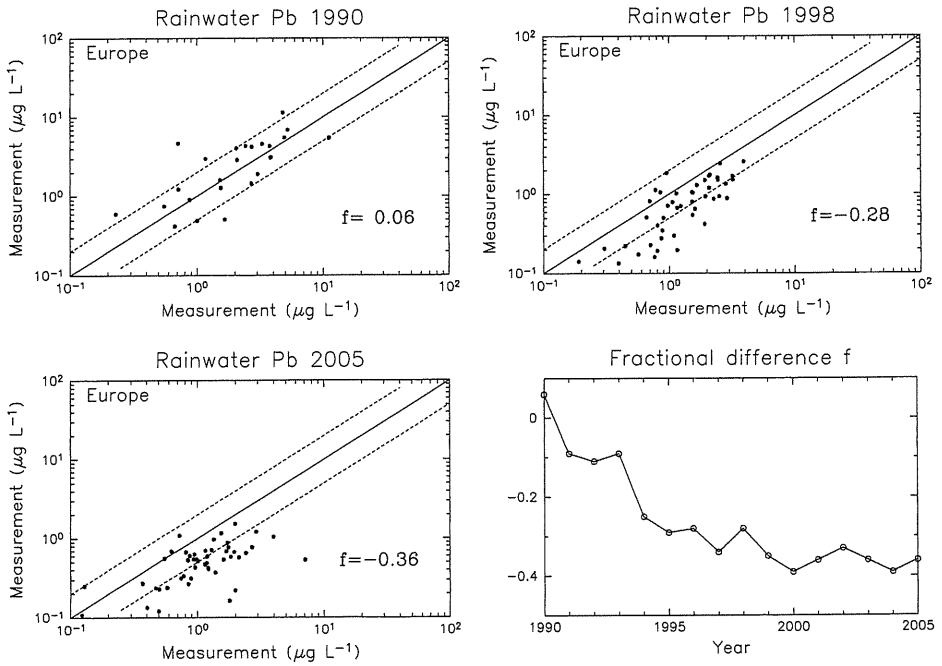

Fig. 5. Scatter plot of the precipitation-weighted concentration in rainwater (μg L^{-1}) over Europe for the model results and observations in 1990, 1998, and 2005. A time series of the *f* value for each year from 1990 to 2005 is also shown. Generally good agreement in the early 1990s and underestimation in 2000s are demonstrated by descending trend of the *f* value. The tendency is similar to that of the surface air.

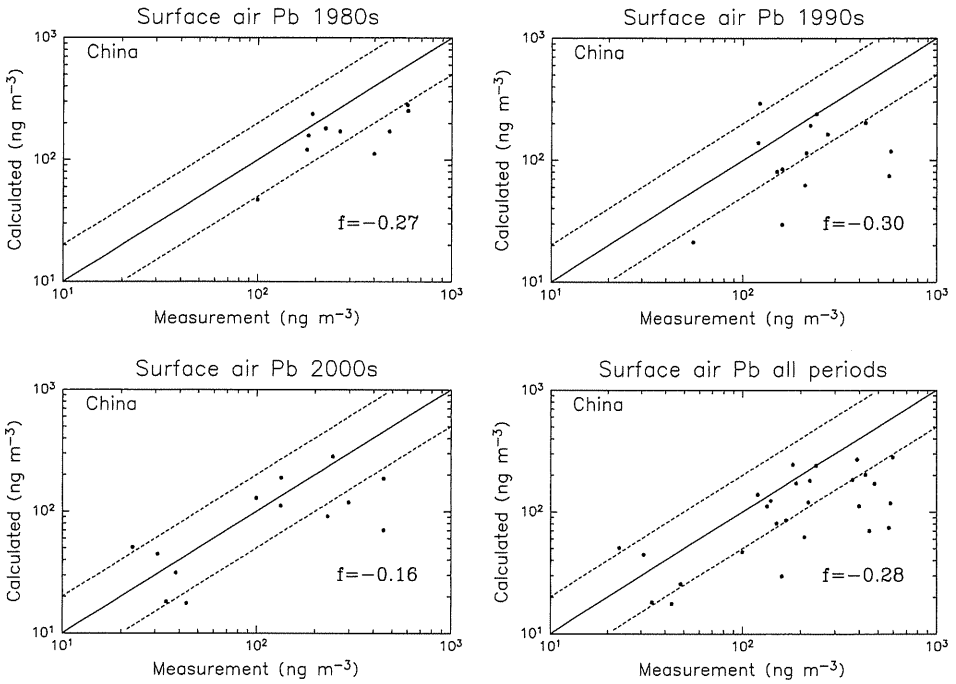

Fig. 6. Scatter plot of lead concentrations (ng m^{-3}) at the surface over China. The plot is for model results and observations from the literature for the 1980s, 1990s, 2000s, and all periods. Calculated concentrations are averaged for the period corresponding to that of the observations. There is a slight underestimation.

period (Fig. 9). The highest concentrations exceed 100 ng m^{-3} in the 1980s, and the concentration decreases to several tens of nanograms per cubic meter in the 2000s. The decline shows the result of emission control efforts, but the present concentration level of surface air lead is somewhat greater than that for Europe.

Calculated concentrations for Korea generally agree with observations from 1991 to 2004 (Fig. 10). Most observed concentrations exceed 100 ng m^{-3} in the early 1990s and decrease significantly later, although they are still about 70 ng m^{-3} in the 2000s and are greater than concentrations observed in Europe and Japan.

3.3. Global budget

The annually averaged global budget (Table 1) shows that most deposition is due to precipitation, reflecting ineffective dry deposition for fine particles with a diameter between 0.1 and 1.0 μm. The residence time in the atmosphere is controlled mainly by wet deposition. The uncertainty of the in-cloud scavenging rate is a factor of 3 for rain and a factor of 6 for snow (Scott, 1982). That of the subcloud scavenging rate is controlled by the collection efficiency between 10^{-3} and 0.7 (Scott, 1978). The range of the residence time is from 1.8 days for the fast deposition case to 4.7 days for the slow deposition case.

Atmospheric lead is emitted at the surface and removed mainly by precipitation. There is no removal process above cloud layers. The residence time averaged over the troposphere is 2.9 days, while it is longer in the upper troposphere (6.3 days above 400 hPa). Larger wind speed makes the spatial scale of transport greater in the upper troposphere. Global-scale transport plays a more important role in the global distribution of deposition flux than in the global distribution of the surface air concentration.

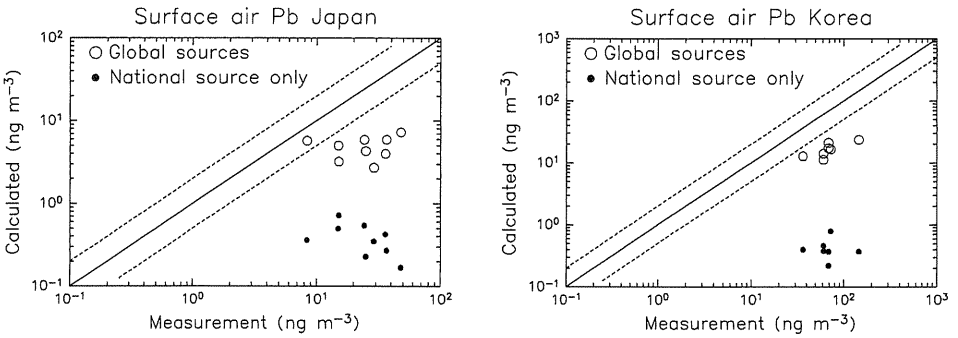

Fig. 7. Scatter plot of lead concentrations (ng m^{-3}) at the surface over Japan and Korea. The plot is for the model results determined using PRTR and TRI and the observations in 2004. (●) and (○) represent calculations including only the national source and those including global sources respectively. A significant underestimation remains even if the transboundary inflow is taken into account.

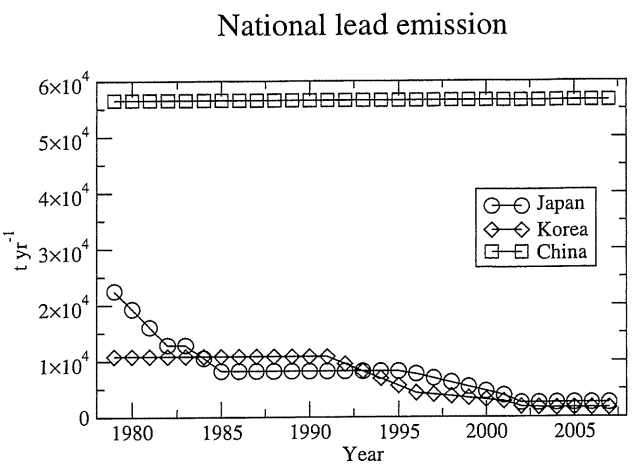

Fig. 8. Time series of the national emission fluxes of lead used in this study (10^3 t yr^{-1}) for Japan, Korea, and China. The emissions for Japan and Korea are optimized using the correction factors. The emission for China is much greater than emissions for Japan and Korea.

4. Discussion

4.1. Sensitivity tests

Sensitivity tests are carried out for the year of 1990. Table 2 shows the variances in the lead burden below a height of about 1 km over the Northern Hemisphere for 50% changes in the meteorological precipitation rate, emission, and major model parameters relating to deposition or diffusion. The sensitivities are for 50% perturbation in one parameter only.

The burden is found to be most sensitive to emission. As lead does not have any chemical production or removal process in the atmosphere, the burden is linear to the emission.

The dominant removal process of atmospheric lead is wet deposition by precipitation as shown in Table 1. The process of wet deposition in the model depends on the meteorological precipitation rate. It has been reported that the precipitation rate of the JRA-25 datasets has a general overestimation of about 10% through comparison with an observation-based estimation of precipitation (Onogi et al., 2007). The sensitivity tests show that a 50% decrease in the large-scale precipitation rate causes only an 11.5% increase in the lead burden.

The lower planetary boundary layer prevents lead ventilation to the free troposphere and consequently increases the burden in the lower layers. A 50% decrease in the height of the boundary layer results in an increase of about 14% in the lead burden of lower layers. The sensitivity to the parameterization of the boundary layer is much lower than that of emission, although it is fairly high. The burden has little sensitivity to other model parameters.

4.2. Lead emission in East Asia

To simulate the distribution of atmospheric lead correctly, both a numerical model with good performance and a reliable dataset of emission are necessary. The performance of the transport model in this work was demonstrated by comparisons with observations in Europe in Section 3.1. Comparison with other models were made in Section 1 of the Supplemental material. The model was

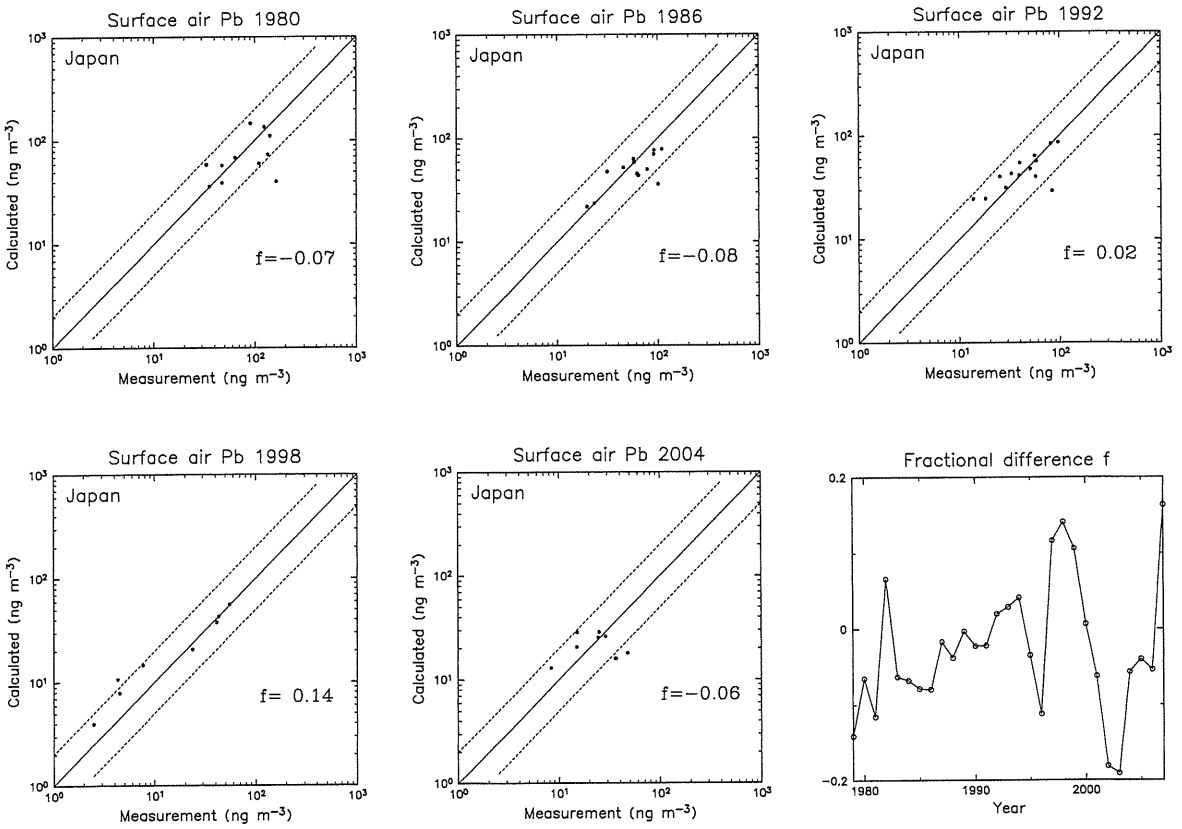

Fig. 9. Scatter plot of annually averaged lead concentrations (ng m^{-3}) at the surface over Japan. The plot is for the model results determined using the optimized emission and observations in 1980, 1986, 1992, 1998, and 2004. A time series of the f value is shown from 1979 to 2007. Fairly good agreement is shown by the f values.

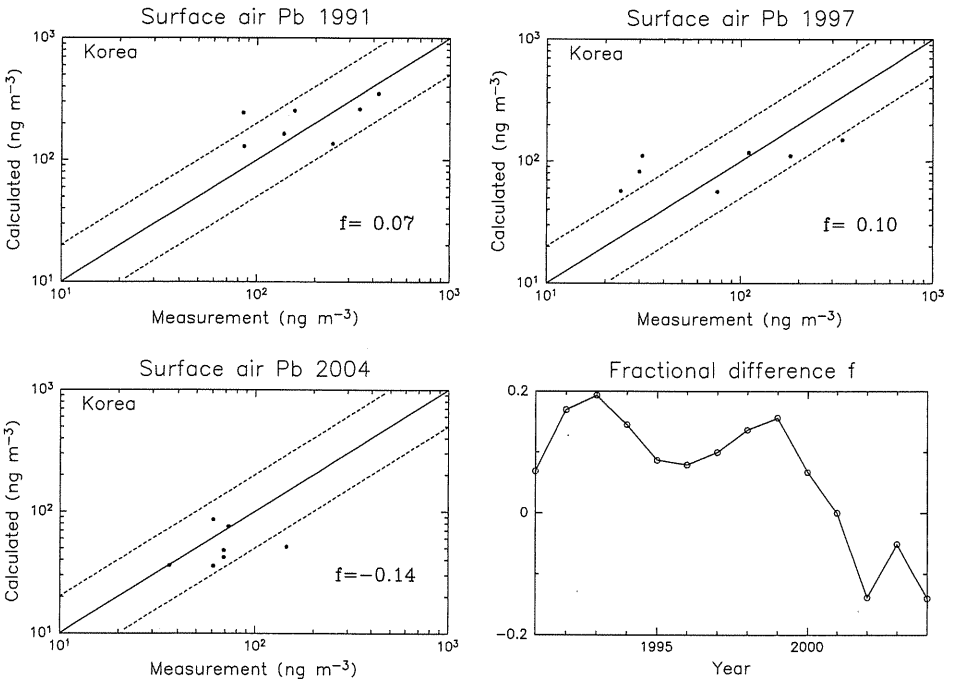

Fig. 10. Scatter plot of annually averaged lead concentrations (ng m^{-3}) at the surface over Korea. The plot is for the model results determined using the optimized emission and observations in 1991, 1997, and 2004. A time series of the f value is shown from 1991 to 2004. Generally good agreement is shown in Korea.

found to make predictions that are somewhat similar to those made by other models.

The sensitivity tests in Section 4.1 show that the model results are most sensitive to emission. Unfortunately, no reliable emission inventory is available for Asia. Therefore, the emissions for the three major countries—China, Korea and Japan—were estimated as described in Section 2.3.1.

Since there is no particular trend in the observed concentrations in China, the emission in China is assumed to have no trend and the emission is derived from economic statistics for a single year, 2001. The calculated surface concentrations in China roughly agree with observations, although there is systematic underestimation as described in Section 3.2. Such underestimation is most likely due to underestimated emission in China. However, the magnitude of the anthropogenic lead emission in China in this work, which is estimated from the economic statistics for 2001 to be 56 000 t yr^{-1} or nearly 4 times the Chinese component in the CGEIC data for 1989, is not small considering the economic scale in China. The discrepancy suggests an unknown source of atmospheric lead in China.

Obviously descending trends are found in observed concentrations in Japan and Korea. Considering that the territories of Japan and Korea are relatively small, the spatial distribution of emission inside each country is fixed at that of the existing emission inventory of CGEIC data described in Section 2.3.1. The magnitude of the annual emission in each year is optimized by multiplying the national annual emission by a correction factor. The correction factors are chosen to minimize the absolute value of the averaged fractional difference, $|f|$. It should be noted that this optimization is based on the assumption that the discrepancy between model results and observations is attributed principally to the magnitude of the national emission.

The national lead emissions in Japan and Korea reported by the PRTR and TRI are less than those in major European countries reported by the EMEP in the 2000s (Tables S3 and S8). On the other hand, observed air concentrations of lead in Japan and Korea are generally higher than those in Europe in the 2000s. As shown by Figs. 4, 9, and 10, representative concentrations are less than 10 ng m^{-3} in Europe, about 20 ng m^{-3} in Japan, and about 60 ng m^{-3} in Korea. The surface air concentrations calculated by the model using the PRTR and TRI data are much less than observations in Japan and Korea as shown in Section 3.2. Although the effect of inflow from windward is significant, the discrepancies are also attributable to underestimations in the inventories. In the PRTR, emissions from the use of materials with the amount of constituent chemical being less than 1% are excused from registration. For example, fossil fuel

Table 1
Annually averaged global budget of lead in the atmosphere for 1990.

Burden	Residence time	Emission	Dry deposition	Wet deposition
1.9 Gg	2.9 days	236 Gg yr^{-1}	3 Gg yr^{-1}	233 Gg yr^{-1}

Table 2
Sensitivity of the lead burden in the lower layer (~1 km) over the Northern Hemisphere to 50% changes in the meteorological precipitation rate, emission, and model parameters for 1990 (%).

	Pr_l	Pr_c	EM	V_{dry}	R_i	R_s	D_h	D_v	H_{pbl}
+50%	−6.3	−2.5	+50.0	−1.1	−4.1	−6.3	−0.2	−2.5	−26.7
−50%	+11.5	+3.6	−50.0	+0.7	+6.1	+9.5	−0.2	+2.3	+13.8

Pr_l: large-scale precipitation rate.
Pr_c: convective precipitation rate.
EM: emission.
V_{dry}: dry deposition velocity.
R_i: in-cloud scavenging rate.
R_s: subcloud scavenging rate.
D_h: horizontal diffusivity.
D_v: vertical diffusivity.
H_{pbl}: planetary boundary layer height.

combustion is excluded in the inventory. Coal consumption for industrial use in Japan is 9×10^7 t yr^{-1} in 2000 (SBJ, 2009), corresponding to lead emission of 900 t yr^{-1} using an emission factor of 10 g t^{-1}. Fossil fuel combustion is included in the emission inventory for Europe reported by the EMEP (EEA, 2009). It is necessary to inspect the frameworks of pollutant registration in Japan and Korea carefully.

It should be noted that observations of atmospheric particles in East Asia have been carried out mainly in urban regions. Although observations affected by particular sources are excluded in evaluating the model as much as possible, effects of particular sources may remain in the observation results. Therefore, observations in remote regions over East Asia are necessary for more detailed model validation. It should also be noted that the samples of atmospheric particles collected in Korea and some of those collected in China include coarse particles. Lead in coarse particles collected near sources could result in underestimation in the model results.

5. Summary

A global atmospheric transport model for lead was developed as a first step in establishing of an assessment system for transboundary air pollutants in East Asia. The results were compared with a large number of observations in East Asia.

First, model validation was carried out by comparison with observations of atmospheric particles and rainwater in Europe. The model results generally agreed well with observations in the 1990s, when anthropogenic emission was dominant.

The anthropogenic emission in China was estimated to be 56 000 t yr^{-1} using economic statistics for 2001. The calculated lead concentrations in the surface air generally agree with observations within a factor of two, although systematic underestimation was found. The underestimation suggests a lack of knowledge about lead emission.

The results obtained using the emission inventories—the PRTR for Japan and TRI for Korea— were much less than the observed lead concentrations in surface air. Those obtained using the optimized emission agreed well with observations.

It is concluded that the transport model in this work reproduces the features of the atmospheric lead distribution in East Asia. In the present study, lead was selected as a model chemical for three reasons. First, there is an accumulated collection of environmental data. Second, the fate of lead is relatively simple since it never degrades in the environment. Third, the toxicological importance of lead is well accepted. The transport model will be applied to other chemicals in the future.

Acknowledgments

This project was supported primarily by the Japan Science and Technology Agency (1300001, 2008–2010). The meteorological datasets used in this study are the JRA-25 long-term reanalysis dataset provided by a cooperative research project of Japan Meteorological Agency and Central Research Institute of Electric Power Industry.

Appendix. Supplementary information

Supplementary data associated with this article can be found, in the online version, at doi:10.1016/j.atmosenv.2010.01.001.

References

Allen, A.G., Nemitz, E., Shi, J.P., Harrison, R.M., Greenwood, J.C., 2001. Size distribution of trace metals in atmospheric aerosols in the United Kingdom. Atmospheric Environment 35, 4581–4591.
EEA, 2009. EMEP/EEA Air Pollutant Emission Inventory Guidebook 2009. EEA Technical report 9/2009. European Environment Agency, Copenhagen, Denmark.
Emde, K.V.D., 1992. Solving conservation laws with parabolic and cubic splines. Monthly Weather Review 120, 482–492.
Feichter, J., Crutzen, P.J., 1990. Parameterization of vertical tracer transport due to deep cumulus convection in a global transport model and its evaluation with ^{222}Radon measurements. Tellus Series B 42, 100–117.
Gong, S.L., 2003. A parameterization of sea-salt aerosol source function for sub- and super-micron particles. Global Biogeochemical Cycles 17 (4), 1097.
Ilyin, I., Rozovskaya, O., Travnikov, O., Aas, W., 2007a. Heavy Metals: Transboundary Pollution of the Environment. EMEP/MSC-E Status Report 2/2007. Meteorological Synthesizing Centre – East of EMEP, Moscow, Russia.
Ilyin, I., Rozovskaya, O., Sokovykh, V., Travnikov, O., 2007b. Atmospheric Modelling of Heavy Metal Pollution in Europe: Further Development and Evaluation of the MSCE-HM Model. EMEP/MSC-E Technical Report 4/2007. Meteorological Synthesizing Centre – East of EMEP, Moscow, Russia.
Kasibhatla, P., Chameides, W.L., St. John, J., 1997. A three-dimensional global model investigation of seasonal variations in the atmospheric burden of anthropogenic sulfate aerosols. Journal of Geophysical Research 102, 3737–3760.
Kim, K.-H., 2007. Airborne lead concentration levels on the Korean peninsula between 1991 and 2004. Atmospheric Environment 41, 809–824.
Kurihara, Y., Holloway Jr., J.L., 1967. Numerical integration of a nine-level global primitive equations model formulated by the box method. Monthly Weather Review 95, 509–530.
Levy II, H., Mahlman, J.D., Moxim, W.J., 1982. Tropospheric N_2O variability. Journal of Geophysical Research 87, 3061–3080.
Louis, J.-F., 1979. A parametric model of vertical eddy fluxes in the atmosphere. Boundary-Layer Meteorology 17, 187–202.
Mahlman, J.D., Moxim, W.J., 1978. Tracer simulation using a global general circulation model: results from a mid-latitude instantaneous source experiment. Journal of the Atmospheric Science 53, 1340–1374.
Onogi, K., Tsutsui, J., Koide, H., Sakamoto, M., Kobayashi, S., Hatsushika, H., Matsumoto, T., Yamazaki, N., Kamahori, H., Takahashi, K., Kadokura, S., Wada, K., Kato, K., Oyama, R., Ose, T., Mannoji, N., Taira, R., 2007. The JRA-25 reanalysis. Journal of Meteorological Society of Japan 85, 369–432.
Pacyna, J.M., Scholtz, M.T., Li Y.-, F., 1995. Global budget of trace metal sources. Environmental Reviews 3, 145–159.
SBJ, 2009. Japan Statistical Yearbook 2009. Statistics Bureau, Ministry of Internal Affairs and Communications, Tokyo, Japan.
Scott, B.C., 1978. Parameterization of sulfate removal by precipitation. Journal of Applied Meteorology 17, 1375–1389.
Scott, B.C., 1982. Theoretical estimates of the scavenging coefficient for soluble aerosol particles as a function of precipitation type, rate and altitude. Atmospheric Environment 16, 1753–1762.
Seinfeld, J.H., Pandis, S.N., 1998. Atmospheric Chemistry and Physics. John Wiley, New York.
Slinn, W.G.N., Hasse, L., Hicks, B.B., Hogan, A.W., Lai, D., Liss, P.S., Munnich, K.O., Sehmel, G.A., Vittori, O., 1978. Some aspects of the transfer of atmospheric trace constituents past the air–sea interface. Atmospheric Environment 12, 2055–2087.
Var, F., Narita, Y., Tanaka, S., 2000. The concentration, trend and seasonal variation of metals in the atmosphere in 16 Japanese cities shown by the results of National Air Surveillance Network (NASN) from 1974 to 1996. Atmospheric Environment 34, 2755–2770.
Vogelezang, D.H.P., Holtslag, A.A.M., 1996. Evaluation and model impact of alternative boundary-layer height formulations. Boundary-Layer Meteorology 81, 245–269.
Williamson, D.L., Rasch, P.J., 1989. Two-dimensional semi-Lagrangian transport with shape-preserving interpolation. Monthly Weather Review 117, 102–129.

Marine Pollution Bulletin 60 (2010) 743–747

Contents lists available at ScienceDirect

Marine Pollution Bulletin

journal homepage: www.elsevier.com/locate/marpolbul

High mercury levels in hair samples from residents of Taiji, a Japanese whaling town

Tetsuya Endo [a,*], Koichi Haraguchi [b]

[a] Faculty of Pharmaceutical Sciences, Health Sciences University of Hokkaido, 1757 Ishikari-Tobetsu, Hokkaido 061-0293, Japan
[b] Daiichi College of Pharmaceutical Sciences, 22-1 Tamagawa-Cho, Minami-Ku, Fukuoka 815-8511, Japan

ARTICLE INFO

Keywords:
Total mercury
Methyl mercury
Hair
Short-finned pilot whale (*Globicephala macrorhynchus*)
Yellowfin tuna
Albacore

ABSTRACT

We investigated the mercury concentrations in red meat from pilot whales consumed by some residents of the Japanese whaling town, Taiji, and in hair samples from 50 residents for their maker of mercury burden. The methyl mercury (M-Hg) level in the red meat was 5.9 μg/wet g, markedly higher than the US FDA action level and Cordex Alimentarius guideline level for predatory fish (1.0 μg/wet g). The average level of total mercury (T-Hg) in the hair from residents who ate whale meat more than once a month was 24.6 μg/g, whereas the average from the residents who did not consume any whale meat was 4.3 μg/g. The T-Hg concentrations in the hair from three donors exceeded 50 μg/g, the level for NOAEL set by WHO. The T-Hg level found in the Taiji whale meat consumers was markedly higher than that observed in the Japanese population overall (about 2 μg/g).

1. Introduction

Mercury (Hg) is distributed through the environment by both natural and anthropogenic processes. Inorganic Hg released into the environment is transformed to organic Hg, mainly in methylated form (methyl mercury; M-Hg), resulting in anthropogenic Hg contamination, and there has been global concern about the high toxicity of M-Hg and its bioaccumulation via the food web (WHO, 1990). In humans, the Hg concentration in hair is the preferred marker for evaluating Hg exposure for a period of several weeks or months (JECFA, 2003). World Health Organization (WHO) concluded that a Hg level of 50 μg/g in human hair corresponds to 'no observed adversary effect level' (NOAEL) of M-Hg for adults, determined by neurotoxicological data (WHO, 1990).

Large epidemiological studies to determine the relationship between maternal exposure to M-Hg and impaired neurological development in children are currently underway in two locations: the Faroe Islands and the Seychelles. Faroe Islanders sometimes eat the meat of long-finned pilot whales (*Globicephala meleanus*) contaminated with high levels of M-Hg, while the Seychelles population, which does not eat whale meat, has a larger intake of fish contaminated with low levels of M-Hg. On the basis of preliminary reports of these studies, the Food and Agriculture Organization (FAO)/WHO Joint Expert Committee on Food Additives (JECFA) lowered its guideline value for provisional tolerable weekly intake (PTWI) of M-Hg from 3.3 μg/kg-bw/week to 1.6 μg/kg-bw/week (JECFA, 2003). By comparison, the US Environmental Protection Agency (US EPA) developed a reference dose (RfD) for M-Hg of 0.1 μg/kg-bw/day (US EPA, 1997). The revised PTWI and RfD correspond to a hair Hg level of 2.2 and 1.0 μg/g, respectively (Yasutake et al., 2004). It is worthy of note that in August 2008, the health authorities in the Faroe Islands revised their recommendations to indicate that long-finned pilot whales are no longer considered fit for human consumption, as the meat and blubber from pilot whales was considered to contain high levels of Hg, PCBs and DDT derivatives as to make it unsafe (Weihe and Joensen, 2008). The revised recommendations suggest that, in addition to damage to fetal neural development, exposure to low levels of Hg could be linked to high blood pressure and impaired immunity in children, as well as increased rates of Parkinson's disease, circulatory problems and possibly infertility in adults (Weihe and Joensen, 2008).

Taiji is a small town of 3400 people (as of 2008) in Wakayama Prefecture, Japan, which has suffered severely from emigration, with about one third of its residents now aged 65 or over (Fig. 1). Taiji is famous as the birthplace of traditional whaling in Japan, and continues the practice of commercial hunting for small cetaceans such as short-finned pilot whales (*Globicephala macrorhynchus*), Risso's dolphins (*Grampus griseus*) and striped dolphins (*Stenella coeruleoalba*). High levels of toxic substances such as heavy metals and organohalogen compounds have been found in the food products from toothed whales, dolphins and porpoises sold for human consumption in Japan, reflecting their position at the top of marine food web and their relative longevity (Haraguchi et al., 2000; Simmonds et al., 2002; Endo et al., 2002, 2003, 2004, 2005). The contamination level of Hg in the red meat from short-finned pilot whales sold in Japan (Endo et al., 2003, 2005) has been shown to be several times higher than that of long-finned pilot whales consumed in the Faroe Islands (Dam and Bloch, 2000). 'Whale meat' (including dolphins and porpoises) remains a

* Corresponding author. Tel./fax: +81 133 23 3902.
E-mail address: endotty@hoku-iryo-u.ac.jp (T. Endo).

0025-326X/$ - see front matter © 2009 Elsevier Ltd. All rights reserved.
doi:10.1016/j.marpolbul.2009.11.020

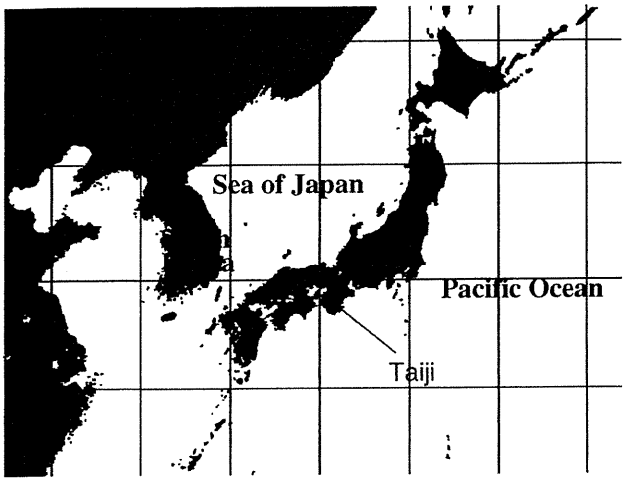

Fig. 1. Map of Japan showing Taiji.

traditional food source enjoyed by many Taiji residents, particularly those residents who making a living from whaling. Furthermore, Taiji residents frequently consume tuna as the town is adjacent to Nachikatsuura, a port famous throughout Japan for its tuna. Although the hazard to the health of Taiji residents from the consumption of whale products is suspicious, no epidemiologic survey has yet been conducted in Taiji.

Here we analyzed the T-Hg and M-Hg in the red meat from small cetaceans (pilot whales and dolphins), slices of fresh tuna (sashimi) and fillets of other fish species marketed in and around Taiji, together with the T-Hg concentrations in the head hair from 50 residents living in Taiji. We then compared the T-Hg concentrations between whale meat consumers and non-consumers, and discussed the possible health problems associated whale meat consumption.

2. Materials and methods

2.1. Sampling of cetacean and fish meats and head hair

The red meat of short-finned pilot whale (*G. macrorhynchus*), striped dolphin (*Stenella coerulecalba*) and Risso's dolphin (*G. griseus*) had purchased from the markets in and around Taiji between 2002 and 2005 (Fig. 1). The sashimi (slices of raw fish) of albacore tuna (*Thunnus alalunga*), yellowfin tuna (*Thunnus albacares*) and skipjack (*Katsuwonus pelamis*), and the fillets of dolphinfish (*Coryphaena hippurus*), ribbonfish (*Trichiurus japonicus*), common head-fish (*Mola mola*), swordfish (*Xiphias gladius*) and striped marline (*Tetrapturus audax*) were also purchased from those markets between 2003 and 2008.

Head hair samples from 50 residents living in Taiji (30 men and 20 women) were collected by local collaborators from among their acquaintances between December 2007 and July 2008. At the time of collection, a simple questionnaire, detailing age, the species consumed, and frequencies of consumption of toothed whales and dolphins per month and tunas and other marine products per week, was completed, along with a declaration of informed consent. The average age of the 50 donors who cooperated in this survey was high (more than 50 years) as expected from the Taiji demographics. No whalers or members of their families, who were presumed to consume a comparatively large amount of pilot whale products, were included in the 50 donors. According to the collaborators' observations, none of the donors showed apparent symptoms of Hg poisoning such as tremble. The hair samples were packed in polyethylene bags and stored at room temperature until analysis.

2.2. Chemical analyses

The total mercury (T-Hg) concentrations in the samples were determined using a flameless atomic absorption spectrophotometer (Hiranuma Sangyo Co. Ltd., HG-1) after digestion by a mixture of HNO_3, HCO_4 and H_2SO_4 (Endo et al., 2002). Methyl mercury (M-Hg) concentrations in the samples were determined using a gas chromatograph (Shimazu Co. Ltd., GC-14A) with a ^{63}Ni electron capture detector (ECD) (Haraguchi et al., 2000). DOLT-2 (National Research Council of Canada) and CRB463 (BCR European Commission) were used as analytical quality control sample for the determination of T-Hg and M-Hg (Endo et al., 2003, 2004). Recoveries of T-Hg and M-Hg were 95% and 85%, respectively.

The concentrations of T-Hg and M-Hg in the red meat and filet samples shown in Table 1 and Fig. 2 were the mean of two or three determinations. The concentration of T-Hg in hair sample was expressed not only by arithmetic mean (AM) ± SD but also geometric mean (GM) with range to compare previous reports.

3. Results

Table 1 shows the contamination levels of T-Hg and M-Hg found in red meat from pilot whales and dolphins, slices of tuna and skipjack, and fillets of other fish species marketed in and around Taiji. As expected, high levels of Hg were found in the red meat from the pilot whales and dolphins. In particular, the contamination levels of T-Hg (9.6 ± 5.3 μg/wet g) and M-Hg (5.9 ± 2.9 μg/wet g) in the red meat from pilot whales were extremely high. Contamination levels of T-Hg and M-Hg in the red meat of striped dolphin were 4.0 ± 3.4 μg/wet g and 2.2 ± 0.8 μg/wet g, respectively, and those of Risso's dolphin were 4.4 ± 2.3 μg/wet g and 3.1 ± 1.7 μg/wet g, respectively. Average concentration of T-Hg in albacore was the same to the T-Hg concentration of the Japanese regulation (0.4 μg/wet g), and that of yellowfin tuna and skipjack were slightly lower than the regulation level. Contamination levels of T-Hg found in swordfish and striped marline were markedly higher than that of tuna, while contamination levels of T-Hg found in dolphinfish, ribbonfish and common head-fish were lower.

According to the results of the questionnaire (Table 2), 39 residents ate red meat from small cetaceans at least once every few months, whereas 11 residents did not eat 'whale meat' at all. Among the 39 residents that were red meat consumers, 28 residents usually ate red meat a few times each month, and 11 residents usually ate it once every few months. The most popular small cetacean species eaten was the short-finned pilot whale. All red meat consumers ate short-finned pilot whale, and some consumers occasionally consumed Risso's and striped dolphins. Many residents ate fresh slices of albacore and/or yellowfin tuna more than once each week, but no resident ate bluefin tuna, probably because of higher price of bluefin tuna. Most of residents ate other species of fish and shellfish at least a few times each week. The frequency of whale meat consumption was higher in males than in females, and all residents who ate whale meat also ate tuna.

The analytical results of T-Hg in hair from the 50 residents are summarized in Fig. 2. The T-Hg concentrations in three residents who ate whale meat more than once each month exceeded the NOAEL (50 μg/g). The highest T-Hg concentration was 67.2 μg/g in a male aged in his 50's. The lowest was 0.4 μg/g in two schoolchildren (aged less than 10 years) who did not eat whale meat or slices of tuna. The average T-Hg concentrations for residents who ate pilot whale and/or dolphin meat more than once each month or once every few months were 24.6 ± 15.6 μg/g (GM and range were 20.4 and 6.6–67.2 μg/g, $n = 28$) and 15.5 ± 10.0 μg/g (GM and range were 13.0 and 4.4–40.2 μg/g, $n = 11$), respectively,

Table 1
Mercury contamination levels in red meat of odontocetes, tunas and other fishes marketed in and around Taiji.

	n	Total mercury (μg/wet g)	Methyl mercury (μg/wet g)
Short-finned pilot whale	22	9.6 ± 5.3 (3.1–21.4)	5.9 ± 2.9 (2.1–12.0)
Striped dolphin	13	4.0 ± 3.4 (1.0–15.7)	2.2 ± 0.8 (1.0–4.1)
Risso's dolphin	19	4.4 ± 2.3 (1.7–9.2)	3.1 ± 1.7 (1.3–8.8)
Albacore	34	0.40 ± 0.12 (0.16–0.75)	N.D.
Yellowfine tuna	21	0.26 ± 0.24 (0.1–1.0)	N.D.
Skipjack	9	0.26 ± 0.17 (0.04–0.54)	N.D.
Dolphinfish	7	0.17 ± 0.09 (0.06–0.30)	N.D.
Ribbonfish	3	0.06 ± 0.03 (0.03–0.09)	N.D.
Common head-fish	6	0.05 ± 0.03 (0.03–0.10)	N.D.
Sword fish	5	1.6 ± 0.24 (0.1–1.0)	N.D.
Striped marline	5	0.78 ± 0.39 (0.32–1.35)	N.D.

The data are shown as mean ± SD with range.
N.D., not determined.

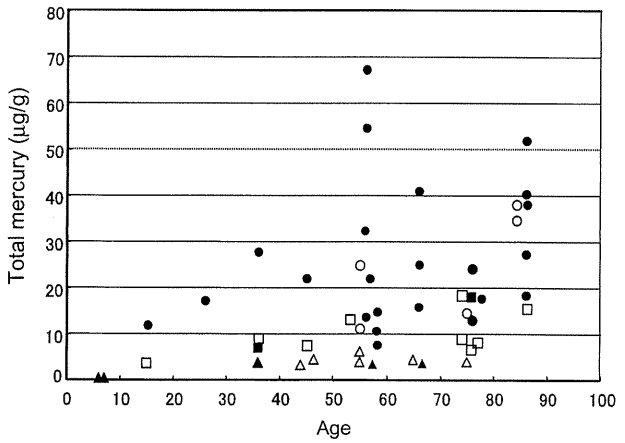

Fig. 2. Mercury concentrations in head hair in the whale meat consumers of Taiji residents. Closed and open symbols represent the mercury concentration in male and female of Taiji residents, respectively. Circle and square represent the whale meat consumers once or more time per month and less than once per month, respectively, and triangle represents the non-consumer.

Table 2
Number and frequency of consumption of red meat from small cetaceans.

Age	Male	Female
0–9	2 (C, C)	0
10–19	1 (A)	1(B)
20–29	1 (A)	0
30–39	3 (A, B,C)	1(B)
40–49	1 (A)	3 (B, C, C)
50–59	9 (A, A, A, A, A, A, A, A, C)	5 (A, A, B, C, C)
60–69	4 (A, A, A, C)	1 (C)
70–79	4 (A, A, A, B)	6 (A, B, B, B, B, C)
80+	5 (A, A, A, A, A)	3 (A, A, B)

A: once or more per month.
B: less than once per month.
C: no consumption.

whereas the average for residents who did not eat pilot whale or dolphin meat at all was 4.3 ± 1.7 μg/g (GM and range were 2.5 and 0.4–6.1 μg/g, $n = 11$). The T-Hg averages of 50 residents, 30 men and 20 women were 17.7 ± 11.5 μg/g (GM was 15.0 μg/g), 21.6 ± 16.7 μg/g (GM was 13.7 μg/g) and 11.9 ± 10.1 μg/g (GM was 9.0 μg/g), respectively. The hair T-Hg concentration tended to increase with age. Among the 50 donors, only one woman was of childbearing age (aged in her 30's, 8.8 μg/g). She ate whale meat once every few months and tuna a few times each week. The hair T-Hg concentrations below 10 μg/g and 20 μg/g were 40% and 70% of 50 donors, respectively.

As data not shown in figure, the hair T-Hg concentration who stopped the eating of pilot whale meat decreased markedly from 33.0 μg/g (December 2007) to 14.7 μg/g (June 2008). This donor was shown in Table 1 as male at 50's with the consumption of "whale meat" once or more time per month.

4. Discussion

4.1. Comparison of hair mercury level of Taiji residents with that of national average

Two research groups had recently conducted the large-scale survey of hair T-Hg concentration in Japan (Yasutake et al., 2004; Yasuda et al., 2005). According to Yasutake et al. (2004), the averages of hair T-Hg concentration (GM) were 2.42 μg/g in male ($n = 4274$) and 1.37 μg/g in female ($n = 4391$) and the total average of male and female was 1.82 μg/g. According to this survey, the percentages below 2.0, 5.0, and 10 μg/g were about 50%, 90%, and 99%, respectively, and the highest concentration was found in a male at 26.76 μg/g. Yasuda et al. (2005) analyzed 5846 hair samples and reported that the GM of hair T-Hg concentration in male adults tended to increase with age from 2.4 μg/g at high-teens up to a peak of 5.9 μg/g at 50's, and then decreased with further aging, and the hair T-Hg level in female was significantly lower than that in male.

In the present survey of hair T-Hg conducted in Taiji, the averages of male and female were 21.6 μg/g (GM was 13.7 μg/g, $n = 30$) and 11.9 μg/g (GM was 9.0 μg/g, $n = 20$), respectively, and the percentage of donors below 10 μg/g was only 40%. These GM values in male and female were about six times higher than those of national average, respectively, and the percentage below 10 μg/g in the Taiji residents (40%) was markedly lower than that in the national average (99%) (Yasutake et al., 2004). The highest concentration of hair T-Hg found in Taiji residents was 67.2 μg/g and the average of hair T-Hg in the male of 50's was 20.3 μg/wet g (GM was 14.0 μg/g, $n = 14$), while corresponding those values reported in the national surveys were 29.37 μg/g (Yasutake et al., 2004) and 5.9 μg/g (Yasuda et al., 2005), respectively. Although the sample size in the present survey was limited ($n = 50$) and the hair samples were not collected using a standardized procedure, the hair T-Hg level in Taiji residents appears to be markedly higher than that in other areas of Japan, and is correlated with frequency of whale meat consumption (Table 2). The hair T-Hg concentration in the Taiji resident who stopped the pilot whale meat consumption was markedly decreased within six months, suggesting that the whale meat is the major intake route for Hg. The half-life of Hg in blood

was reported to be about 70 days (Miettinen et al., 1971). The Taiji residents who make their living from whaling are expected to consume much more whale meat and to have higher hair T-Hg levels, but none of those residents were included among the 50 donors.

4.2. Risk assessment of mercury exposure due to the whale consumption in Taiji residents

Contamination levels of M-Hg in the red meats of short-finned pilot whale, striped and Risso's dolphins were markedly higher than the US FDA action level and Cordex Alimentarius guideline level of M-Hg in predatory fish (1.0 μg/wet g). Based on the present data of M-Hg concentration in the red meat of short-finned pilot whale (5.9 μg/wet g), consumption of only 17 g and 8 g of the red meat per one week exceeds the PTWI and the RfD of M-Hg per 60 kg, respectively. The whale meat consumers in Taiji also appear to preferentially consume tuna and other fish species, and most of whale meat consumers in Taiji appear to intake M-Hg exceed the PTWI and the RfD. The intake of M-Hg at PTWI (1.6 μg/kg/week) set by JECFA (2003) corresponds to a hair T-Hg concentration of 2.2 μg/g (Yasutake et al., 2004). Only two donors in the present survey (school children) were below this T-Hg level. The highest concentration of 67.2 μg/g found in the present survey corresponds to about 31 times of the PTWI. The hair T-Hg concentration of 20.4 μg/g (the average of the pilot whale meat consumers more than once in every month) corresponds to the consumption of 150 g of the pilot whale meat (5.9 μg/wet g) per one week, exceeding 9.3 times the PTWI. According to the questionnaire, however, no donor ate the whale and dolphin meats more than once per week. Therefore, the consumption of tunas and other fish species may contribute to the high concentration of hair T-Hg in the Taiji residents known to consume whale meat. The Hg levels of tunas and other fish species shown in Table 1 are comparable to those in previous reports (Yamashita et al., 2005; Kojadinovic et al., 2006; Kaneko and Ralston, 2007).

4.3. Comparison of mercury levels of hair and whale meat in the Faroe Islands

As mentioned in Introduction, the health authorities in the Faroe Islands revised their recommendations to indicate that long-finned pilot whales are no longer considered fit for human consumption, as the meat and blubber from pilot whales was considered to contain high levels of Hg, PCBs and DDT derivatives (Weihe and Joensen, 2008). Choi et al. (2009) suggested that the increased M-Hg intake from pilot whale meat promoted the development of cardiovascular disease of Faroese whaling men. They reported that the current level of T-Hg (GM) in the hair of Faroese whaling men was 7.31 μg/g (0.92–46.0 μg/g, $n = 42$) and more than half of the men ate the whale meat three or more time each month (Choi et al., 2009). The hair T-Hg level of the Taiji residents (GM was 15.0 μg/g, $n = 50$) was higher than that of the Faroese whaling men. The Taiji residents may be eating the whale red meat more polluted by Hg, because levels of T-Hg and M-Hg found in the short-finned pilot whales sold in and around Taiji (Table 1) were a few times higher than those in the long-finned pilot whales caught off Faroe Islands (Julshamn et al., 1987; Dam and Bloch, 2000). In addition, Taiji residents tend to preferentially eat albacore and yellowfin tunas and other fish species. Furthermore, contamination levels of PCBs and other organohalogen compounds fund in whale products sold in and around Taiji (Haraguchi et al., 2000; Simmonds et al., 2002) were compatible levels to those reported in the Faroe Islands (Dam and Bloch, 2000). The large-scale survey of hair T-Hg concentration in Taiji residents is necessary to prevent the health problems associated with the consumption of whale products.

4.4. Comparison of mercury levels in hair due to the fish consumption

Apart from Japan, hair Hg levels associated with the consumption of marine food have been surveyed in China and Indonesia (Feng et al., 1998), US (McDowell et al., 2004), Cambodia (Agusa et al., 2005), Morocco (Elhamri et al., 2007) and Malaysia (Hajeb et al., 2008). According to those studies, the hair Hg levels in populations (GM) with little or no fish consumption were below 0.5 μg/g (McDowell et al., 2004), and the averages (AM or GM) among fish consumers increased by up to about 15 μg/g in proportion to the level of fish consumption (Hajeb et al., 2008). To our knowledge, no hair Hg exceeding 50 μg/g (NOAEL) has yet been reported in fish consumers. In contrast, the T-Hg concentrations in the hair from three residents who ate the whale meat more than once each month exceeded 50 μg/g (Fig. 2). Choi et al. (2009) reported the hair T-Hg concentration of 54.1 μg/g in a Faroese whaling men. Extremely high level of hair Hg (705 μg/g) was reported in a patient of Minamata disease who ate fish contaminated with anthropogenic origin of Hg (Harada, 1995).

Acknowledgments

We deeply appreciate the assistances provided by Mr. Jun-ichiro Yamashita in sampling the hair from Taiji residents and Dr. C.S. Baker, Oregon State University, for critical reading the manuscript. This work was supported by a Grant-in-Aid from the Japan Society of for the Promotion of Science (C18602002).

References

Agusa, T., Kunito, T., Iwata, H., Monirith, I., Tana, T.S., Shbramanian, A., Tanabe, S., 2005. Mercury contamination in human hair and fish from Cambodia: levels, specific accumulation and risk assessment. Environ. Pollut. 134, 79–86.

Choi, A.L., Whihe, P., Budtz-Jœrgensen, E., Jœrgensen, P.J., Salonen, J.T., Tuomainen, T-P., Murata, K., Nielsen, H.P., Petersen, M.S., Askham, J., Grandjean, P., 2009. Methylmercury exposure and adverse cardiovascular effects in Faroese whaling men. Environ. Health Perspect. 117, 367–372.

Dam, M., Bloch, D., 2000. Screening of mercury and persistent organochlorine pollutants in long-finned pilot whale (*Globicephala melas*) in the Faroe Islands. Mar. Pollut. Bull. 40, 1090–1099.

Elhamri, H., Idrissi, L., Coquery, M., Azemard, S., El Abide, A., Benlemlin, M., Saghi, M., Caubadda, F., 2007. Hair mercury levels in relation to fish consumption of the Moroccan Mediterranean coast. Food Addit. Contam. 24, 1236–1246.

Endo, T., Haraguchi, K., Sakata, M., 2002. Mercury and selenium concentrations in the internal organs of toothed whales and dolphins marketed for human consumption in Japan. Sci. Total Environ. 300, 15–22.

Endo, T., Hotta, Y., Haraguchi, K., Sakata, M., 2003. Mercury contamination in the red meat of whales and dolphins marketed for human consumption in Japan. Environ. Sci. Technol. 37, 2681–2685.

Endo, T., Haraguchi, K., Cipriano, F., Simmonds, M.P., Hotta, Y., Sakata, M., 2004. Contamination by mercury and cadmium in the cetacean products from Japanese market. Chemosphere 54, 1653–1662.

Endo, T., Haraguchi, K., Hotta, Y., Hisamichi, Y., Lavery, S., Dalebout, M.L., Baker, C.S., 2005. Total mercury, methyl mercury, and selenium levels in the red meat of small cetaceans sold for human consumption in Japan. Environ. Sci. Technol. 39, 5703–5708.

Feng, Q., Suzuki, Y., Hisashige, A., 1998. Hair mercury levels of residents in China, Indonesia, and Japan. Arch. Environ. Health 53, 36–43.

Hajeb, P., Selamat, J., Ismail, A., Baker, F.A., Baker, J., Lioe, H.N., 2008. Hair mercury level of coastal communities in Malaysia: a linkage with fish consumption. Eur. Food Res. Technol. 225, 1349–1355.

Harada, M., 1995. Minamata disease: methylmercury poisoning in Japan caused by environmental pollution. Crit. Rev. Toxicol. 25, 1–24.

Haraguchi, K., Endo, T., Sakata, M., Masuda, Y., 2000. Contamination survey of heavy metals and organochlorine compounds in cetacean products purchased in Japan. J. Food Hyg. Soc. Jpn. 41, 287–296.

JECFA, 2003. Summary and Conclusions of the 61st Meeting of the Joint FAO/WHO Expert Committee of Food Additives (JECFA), JECFA/61/SC. Rome, Italy.

Julshamn, K., Andersen, A., Ringdal, O., Mørkøre, J., 1987. Trace elements intake in the Faroe Islands I. Element levels in edible parts of pilot whales (*Globicephala melas*). Sci. Total Environ. 65, 53–62.

Kaneko, J.J., Ralston, N.V., 2007. Selenium and mercury in pelagic fish in the Central North Pacific near Hawaii. Biol. Trace Elem. Res. 119, 242–254.

Kojadinovic, J., Potier, M., Le Corre, M., Cosson, R.P., Bustamante, P., 2006. Mercury content in commercial pelagic fish and its risk assessment in the Western Indian Ocean. Sci. Total Environ. 366, 688–700.

McDowell, M.A., Dillon, C.F., Osterloh, J., Bolger, M., Pellizzari, E., Fernando, R., De Oca, R.M., Schober, S.E., Sinks, T., Jones, R.L., Mahaffey, K.R., 2004. Hair mercury levels in US children and women of childbearing age: reference range data from NHANES 1999–2000. Environ. Health Perspect. 112, 1165–1171.

Miettinen, J.K., Rahola, T., Hattula, T., Rissanen, K., Tillander, M., 1971. Elimination of ^{203}Hg-methylmercury in man. Ann. Clin. Res. 3, 116–122.

Simmonds, M.P., Haraguchi, K., Endo, T., Cipriano, F., Palumbi, S.R., Troisi, G.M., 2002. Human health significance of organochlorine and mercury contaminations in Japanese whale meat. J. Toxicol. Environ. Health A 65, 1211–1235.

US EPA, 1997. Mercury Study Report to Congress. EPA, Washington, DC.

Weihe, P., Joensen, H.D., 2008. Recommendations to the government of the Faroe Islands concerning the pilot whale, English translation. <http://www.chef-project.dk/PDF/Medical_Recom_Whale.pdf->.

WHO, 1990. Environmental Health Criteria 101: Methylmercury. WHO, Geneva.

Yamashita, Y., Omura, Y., Okazaki, E., 2005. Total mercury and methylmercury levels in commercially important fishes in Japan. Fish Sci. 71, 1029–1035.

Yasuda, H., Yoneshiro, T., Yoshida, K., Shibazaki, T., Ishii, T., Tsutsui, T., 2005. High toxic metal levels in scalp hair of infants and children. Biomed. Res. Trace Elem. 16, 39–45.

Yasutake, A., Matsumoto, M., Yamaguchi, M., Hachiya, N., 2004. Current hair mercury levels in Japanese for estimation of methylmercury exposure. J. Health Sci. 50, 120–125.

Environ. Sci. Technol. **2010,** *44,* 2675–2681

Stable Isotope Ratios of Carbon and Nitrogen and Mercury Concentrations in 13 Toothed Whale Species Taken from the Western Pacific Ocean off Japan

TETSUYA ENDO,*,† YOHSUKE HISAMICHI,† OSAMU KIMURA,† KOICHI HARAGUCHI,‡ SHANE LAVERY,§ MEREL L. DALEBOUT,|| NAOKO FUNAHASHI,⊥ AND C. SCOTT BAKER#

Faculty of Pharmaceutical Sciences, Health Sciences University of Hokkaido, 1757 Ishikari-Tobetsu, Hokkaido 061-0293, Japan, Daiichi College of Pharmaceutical Sciences, 22-1 Tamagawa-Cho, Minami-Ku, Fukuoka 815-8511, Japan, School of Biological Sciences, University of Auckland, Private Bag 92019, Auckland, New Zealand, School of Biological, Earth and Environmental Sciences, University of New South Wales, Sydney, New South Wales 2052, Australia, International Fund for Animal Welfare, 1-6-10-203, Saiwaicho, Higashikurume, Tokyo 203-0052, Japan, and Marine Mammal Institute and Department of Fisheries and Wildlife, Oregon State University, Newport, Oregon 97365

Received November 27, 2009. Revised manuscript received January 29, 2010. Accepted February 17, 2010.

Stable isotope ratios of carbon ($\partial^{13}C$) and nitrogen ($\partial^{15}N$) and total mercury (T-Hg) concentrations were measured in red meat samples from 11 odontocete species (toothed whales, dolphins, and porpoises) sold in Japan ($n = 96$) and in muscle samples from stranded killer whales ($n = 6$) and melon-headed whales ($n = 15$), and the analytical data for these species were classified into three regions (northern, central, and southern Japan) depending on the locations in which they were caught or stranded. The $\partial^{15}N$ in the samples from southern Japan tended to be lower than that in samples from the north, whereas both $\partial^{13}C$ and T-Hg concentrations in samples from the south tended to higher than those in samples from northern Japan. Negative correlations were found between the $\partial^{13}C$ and $\partial^{15}N$ values and between the $\partial^{15}N$ value and T-Hg concentrations in the combined samples all three regions ($\gamma = -0.238$, $n = 117$, $P < 0.01$). The $\partial^{13}C$, $\partial^{15}N$, and T-Hg concentrations in the samples varied more by habitat than by species. Spatial variations in $\partial^{13}C$, $\partial^{15}N$, and T-Hg concentrations in the ocean may be the cause of these phenomena.

1. Introduction

Stable isotope analyses have been used as an alternative to stomach content analysis to obtain information on the feeding ecology of marine species (*1*–*4*). The $\partial^{13}C$ value is used to indicate the relative contribution to the diet of potential primary sources and can demonstrate differences between pelagic and benthic prey species (*5*–*7*). Furthermore, the $\partial^{13}C$ value in marine phytoplankton decreases slightly from the equatorial regions toward the North Pole at about 0.015 ‰ per 1° (*8*), and this decrease is consequently reflected in the $\partial^{13}C$ values in marine predators. On the other hand, the $\partial^{15}N$ value shows a stepwise increase in the trophic level of a food chain. A significant increase in $\partial^{15}N$ of 3.4 ± 1.1‰ has been shown to occur between consumer and prey (*9*), whereas only a small enrichment of about 1‰ is found in the $\partial^{13}C$ value (*10*). Variations in $\partial^{15}N$ also reflect the regional characteristics of nitrogen metabolism such as denitrification and N_2 fixation (*6*, *11*).

The main islands of Japan are surrounded by a number of both warm and cold ocean currents (Figure 1). Tanaka et al. (*7*) analyzed the $\partial^{13}C$ and $\partial^{15}N$ in Japanese anchovy (*Engraulis japonicus*) samples from the Pacific coast: They reported higher values from inshore samples than from offshore samples and lower values from anchovies taken from the Kuroshio (warm current) extension and Kuroshio-Oyashio (cold current) transition zones. However, little is known about the $\partial^{13}C$ and $\partial^{15}N$ in marine samples taken from northern Japan (cold current region). According to a worldwide survey of squid (*6*), the $\partial^{13}C$ ranges from −19.9 ‰ to −13.8 ‰ and the $\partial^{15}N$ ranges from 8.3 ‰ to 16.8 ‰, with the lowest $\partial^{13}C$ values found in squid caught in the Sea of Japan.

The Japanese archipelago stretches for more than 3000 km from north to south, and many species of toothed whales, including dolphins and porpoises, are known to inhabit the coastal waters. About 20,000 of those cetaceans are annually caught off the coast of Japan for human consumption. The main species of small cetaceans taken are Dall's porpoise (*Phocoenoides dalli*), Baird's beaked whale (*Berardius bairdii*), short-finned pilot whale (*Globicephala macrorhynchus*), pantropical spotted dolphin (*Stenella attenuata*), Risso's dolphin (*Grampus griseus*), rough-toothed dolphin (*Steno bredanensis*), striped dolphin (*Stenella coeruleoalba*), common bottlenose dolphin (*Tursiops truncatus*), and false killer whale (*Pseudorca crassidens*) (*12*). Baird's beaked whales are caught off Abashiri, Hakodate, Ayukawa (Ishinomaki), and Wada (Minamiboso), northern form short-finned pilot whales are caught off Ayukawa, and southern form short-finned pilot whales are caught off Wada, Taiji, and Nago (Figure 1). Dall's

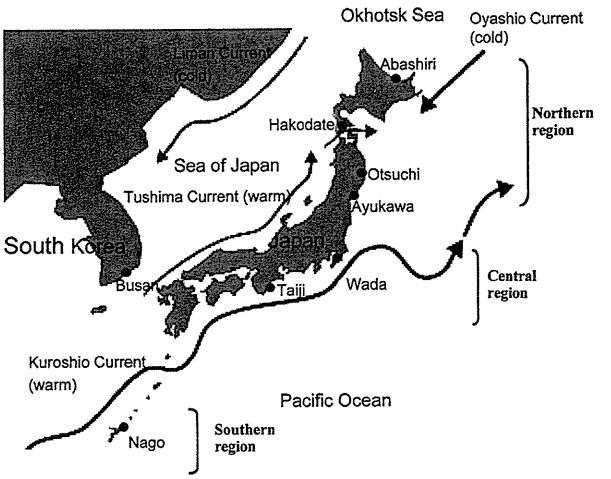

FIGURE 1. Map of Japan and South Korea showing warm and cold currents and whaling towns.

* Corresponding author phone and fax: +81-133-23-3902; e-mail: endotty@hoku-iryo-u.ac.jp.
† Health Sciences University of Hokkaido.
‡ Daiichi College of Pharmaceutical Sciences.
§ University of Auckland.
|| University of New South Wales.
⊥ International Fund for Animal Welfare.
Oregon State University.

10.1021/es903534r
Published on Web 03/10/2010

porpoises are mainly caught off Otsuchi, and other cetacean species are mainly caught off Taiji and/or Nago. Abashiri (N44° and E144°) is the northernmost and Nago (N26° and E128°) is the southernmost of these whaling towns.

As small cetaceans are long-lived and occupy the top of the marine food web, they biomagnify marine pollutants such as heavy metals and organochlorine compounds (*12*–*15*). Among these pollutants, accumulation of mercury (Hg) is prominent, and high levels of Hg are found in red meat products from small cetaceans sold in Japan. To date, the highest and second highest concentrations of total mercury (T-Hg) found in our laboratory were 98.9 and 81.0 μg/wet g in red meat products from a bottlenose dolphin (*15*) and a false killer whale (*12*), respectively. These products were purchased in Nago, the southernmost whaling town in Japan. The T-Hg contamination levels in small cetaceans caught off the coast of Japan vary markedly by the species (*12, 15, 16*) and by habitat (*12, 17*).

The level of Hg accumulation is generally correlated with trophic level as determined by $\partial^{15}N$ value (*18*). However, there are often wide intraspecific and/or interspecific variations in $\partial^{15}N$ within a similar trophic level, and it has been suggested that this results from geographical variations as mentioned above (*6, 7, 11*). We previously reported the contamination level of T-Hg in red meat products from nine species of odontocetes (*12, 15*). However, little is known about the $\partial^{13}C$ and $\partial^{15}N$ values in those species or the correlation between T-Hg concentration and $\partial^{15}N$ in those species.

Killer whales (*Orcinus orca*) represent the top of marine food web and have the most diverse diet, ranging from fish/squid of all sizes to seals and other cetacean species (*19*). In the eastern North Pacific Ocean, three sympatric forms of killer whales, referred to as "residents", "transients" and "offshore", with fundamentally different dietary preferences have been described (*3*). Resident killer whales principally consume marine fish while transient killer whales generally hunt marine mammals (*3*). Reflecting their dietary preferences, contamination level of organohalogen compounds in the blubber and the $\partial^{15}N$ value in the skin of transients were higher than those of residents, respectively (*3*). In contrast to killer whales in the eastern North Pacific Ocean, information about the feeding habits and migration of killer whales in the western North Pacific Ocean is very limited. Available data for killer whales in this area are limited to the T-Hg distribution in the organs of killer whales stranded on the coast of Hokkaido, in the north of Japan (*17*). From stomach content analysis, these killer whales appear to correspond to the transient form. However, the contamination level of T-Hg in these killer whales was low compared to that in other odontocetes caught off the coast of Japan (*17*). In 2006, a pod of melon-headed whales (*Peponocephala electra*) was mass-stranded on the coast of Chiba Prefecture, in central Japan. We analyzed heavy metals in the organs of the stranded whales and reported that the T-Hg concentrations in the organs increased with their body lengths (*20*). To our knowledge, however, stable isotopes ratios in the muscle of neither killer whales nor melon-headed whales around the coast of Japan have yet been reported.

Here, we reported on the stable isotope ratios of carbon ($\partial^{13}C$) and nitrogen ($\partial^{15}N$) and the T-Hg concentration in the red meat products from 11 species of odontocetes purchased from several Japanese whaling towns and their environs as published previously. Furthermore, we analyzed stable isotope ratios and T-Hg concentration in muscle samples from stranded killer whales and melon-headed whales. We compared the $\partial^{13}C$, $\partial^{15}N$, and the T-Hg concentration in the red meat (muscle) samples among whaling towns by area (northern, central, and southern Japan) and among species and investigated the correlation among the $\partial^{15}N$ and $\partial^{13}C$ values and T-Hg concentration.

2. Materials and Methods

2.1. Red Meat Products and Muscle Samples Originating from Odontocetes. As reported previously (*12, 14, 15*), 88 samples of red meat products were purchased from retail outlets in Japan from 2000 to 2004 and analyzed for total mercury (T-Hg) concentration as well as species identification using molecular taxonomy. These samples were analyzed for determination of $\partial^{13}C$ and $\partial^{15}N$ (see below). Eight samples of red meat products purchased in 2004 and 2005 were analyzed for the determination of $\partial^{13}C$, $\partial^{15}N$, and T-Hg concentration and identification of species origin. Muscle samples from mature killer whales stranded on the coast of Hokkaido Prefecture, in northern Japan ($n = 6$) (*17*), and mature melon-headed whales stranded on the coast of Chiba Prefecture, in central Japan ($n = 15$) (*20*), were also analyzed for $\partial^{13}C$ and $\partial^{15}N$. All products were stored at −20 °C prior to analyses.

2.2. Chemical Analyses. The T-Hg concentrations in the odontocete products were determined using a flameless atomic absorption spectrophotometer (Hiranuma Sangyo, HG-1, Japan) after digestion by a mixture of HNO_3, $HClO_4$, and H_2SO_4 (*12, 21*). The species of origin of odontocete products was identified from the mitochondrial DNA sequences (*22*).

After the removal of lipid using chloroform/methanol, the stable isotope ratios of carbon and nitrogen ($\partial^{13}C$ and $\partial^{15}N$) in the dried red meat (muscle) samples were analyzed using a mass spectrometer (Delta S, Finnigan Co., Germany) coupled with an elemental analyzer (EA1108, Fisons Co., Italy) (*4*).

2.3. Statistical Analyses. The data were analyzed using the Statcell 12 program, and the level of significance was set at $P < 0.05$. All data were expressed as the mean ± standard deviation (S.D.).

3. Results

Measurements of $\partial^{13}C$ and $\partial^{15}N$ were obtained from 88 samples of red meat products from 11 cetacean species and 21 muscle samples from stranded mature killer whales and mature melon-headed whales. These samples, representing 13 species, were stratified into northern, central, and southern regions on the basis of the locations of the whaling towns and stranding areas from which they were obtained (Table 1). The northern and southern form pilot whales were stratified by the area in which the samples were purchased. Although the southern form short-finned pilot whales are caught off Wada and Taiji (central Japan) as well as Nago (southern Japan) (Figure 1), we classified all samples from southern form short-finned pilot whale in the central region. As the northern form short-finned pilot whales are caught off Ayukawa, samples from this type were classified into the northern region. As Baird's beaked whales are caught off Abashiri, Hakodate, and Ayukawa (northern Japan) as well as Wada (central Japan) and striped dolphins are caught off Taiji (central Japan) and Nago (southern Japan), we classified the samples from these whales into the northern and central regions, respectively, based on purchase location.

Among the 13 species shown in Table 1, the four lowest average T-Hg concentrations were found in Baird's beaked whale, the northern form short-finned pilot whale, Dall's porpoise, and killer whale. All those species were found in the northern region, and average values of T-Hg concentrations were about 1.3 μg/wet g. In contrast, all average T-Hg concentrations in the red meat (muscle) samples of whales and dolphins found in the central and southern regions exceeded 3.0 μg/wet g. High but variable concentrations of T-Hg were found in the red meat products of bottlenose dolphins and false killer whales. The highest and second highest concentrations in the red meat products summarized

TABLE 1. Stable Isotope Ratios of Carbon and Nitrogen and Total Mercury Concentration in the Red Meat Products and Muscle Samples of Odontocetes Caught off the Coast of Japan

group	species	mean ± SD		
		$\delta^{13}C$ (‰)	$\delta^{15}N$ (‰)	total mercury (μg/wet g)
Northern	killer whale[a] (n = 6)	−17.1 ± 0.1	16.5 ± 0.3	1.27 ± 0.13
	Baird's beaked whale (n = 19[b])	−17.8 ± 0.6	16.3 ± 0.8	1.30 ± 0.99
	short-finned pilot whale, northern form (n = 5)	−18.3 ± 0.6	13.3 ± 0.8	1.30 ± 0.41
	Dall's porpoise (n = 8)	−18.8 ± 0.2	13.2 ± 0.3	1.27 ± 0.33
Central	striped dolphin (n = 11[b])	−17.7 ± 0.6	12.3 ± 0.9	5.91 ± 4.07
	Risso's dolphin (n = 8)	−16.7 ± 0.3	13.1 ± 0.5	3.84 ± 1.52
	short-finned pilot whale, southern form (n = 18[b])	−16.9 ± 0.5	12.2 ± 0.7	12.4 ± 8.6
	melon-headed whale[a] (n = 15)	−16.8 ± 0.2	12.7 ± 0.3	4.89 ± 2.32
	bottlenose dolphin (n = 10)	−17.2 ± 0.3	13.1 ± 0.6	38.3 ± 28.3
Southern	pygmy killer whale (n = 2)	−17.6	14.1	13.1
	false killer whale (n = 5)	−16.2 ± 0.6	12.8 ± 0.6	20.7 ± 10.6
	pantropical spotted dolphin (n = 4)	−17.3 ± 0.3	12.1 ± 0.8	5.33 ± 1.75
	rought-toothed dolphin (n = 6)	−16.9 ± 0.5	11.6 ± 0.5	5.33 ± 1.75

[a] Muscle from stranded animals. [b] Sum of Baird's beaked whales purchased in and around Abashiri, Hakodate, Ayukawa, and Wada, sum of short-finned pilot whales (southern form) purchased from in and around Taiji and Nago, or sum of striped dolphins purchased in and around Taiji and Nago.

in Table 1 were 65.3 μg/wet g in sample from bottlenose dolphins and 32.3 μg/wet g in sample from false killer whales purchased in Nago (southern Japan).

Among the 13 species, excluding the pygmy killer whale (n=2), the average $\partial^{15}N$ in the four species from the northern region was the four highest (Table 1). In contrast, the average $\partial^{13}C$ values from the species in the northern region, excluding the killer whale, were the three lowest. The $\partial^{13}C$-$\partial^{15}N$ map of four species in the northern region appeared to be different from that of nine species in the central and southern regions (Figure 2). The $\partial^{13}C$ tended to increase with increases in the $\partial^{15}N$ among the four species from the northern region (P < 0.01), whereas no correlation was found between the $\partial^{15}N$ and T-Hg concentration (P > 0.05).

The $\partial^{15}N$ of nine species from the central and southern regions tended to be lower than that of the four species from the northern region, whereas the $\partial^{13}C$ of the former region tended to be higher (Figure 2). No correlations (P > 0.05) were found between the $\partial^{13}C$ and $\partial^{15}N$ values and between the $\partial^{15}N$ and T-Hg concentration in the whales and dolphins from the central and southern regions.

It is noteworthy that negative correlations were found between the $\partial^{13}C$ and $\partial^{15}N$ values ($\gamma = -0.223$, $P < 0.05$) and the $\partial^{15}N$ value and T-Hg concentration ($\gamma = -0.238$, $P < 0.01$) in the combined samples from all three regions (n = 117), while positive correlation was found between the $\partial^{13}C$ value and T-Hg concentration ($\gamma = 0.219$, n = 117, $P < 0.05$). These correlations were weak but statistically significant.

The T-Hg concentration and the $\partial^{13}C$ and $\partial^{15}N$ in the Baird's beaked whale products purchased in and around Abashiri, Hakodate, Ayukawa, and Wada were compared (Table 2, see Figure S1). In agreement with the results shown in a previous report (*12*), the T-Hg concentrations in Baird's beaked whale products purchased in and around Abashiri were significantly lower than those in products purchased in and around Ayukawa and Wada (P < 0.05). The $\partial^{15}N$ value from beaked whale products purchased in and around Hakodate was significantly lower than those in products purchased in and around Ayukawa and Wada (P < 0.05), and the $\partial^{13}C$ values from whale products purchased in and around Abashiri and in and around Hakodate were significantly lower than those from the products purchased in and around Ayukawa and Wada (P < 0.05).

The T-Hg concentration, $\partial^{13}C$ and $\partial^{15}N$ in the short-finned pilot whales caught off Ayukawa (northern form), and Taiji and Nago (southern form) were also compared (Table 2, see Figure S2). Again, in agreement with the results of a previous report (*12*), the T-Hg concentrations in red meat products of pilot whales purchased in and around Ayukawa were significantly lower than that in the products purchased in and around Nago (P < 0.05). Correspondingly, the $\partial^{15}N$ values of the products purchased in and around Nago were significantly lower than those from the products purchased in and around Ayukawa (P < 0.05), and the $\partial^{13}C$ values of the products purchased in and around Ayukawa were significantly lower than those of products purchased in and around Taiji and Nago (P < 0.05). On the other hand, no differences were found in the $\partial^{13}C$ and $\partial^{15}N$ values or T-Hg concentrations in red meat products from striped dolphins caught off Taiji and Nago (Table 2).

4. Discussion

4.1. Geographical Differences in $\partial^{13}C$, $\partial^{15}N$, and Hg Contamination. The $\partial^{13}C$ and $\partial^{15}N$ values of red meat (muscle) samples of four species from the northern area of Japan were apparently lower and higher than those of other species from the central and southern areas, respectively (Figure 2). The $\partial^{13}C$ values in the combined samples of northern, central, and southern regions tended to decrease with an increase in $\partial^{15}N$ ($\gamma = -0.223$, n = 117, $P < 0.05$). To explain this negative correlation, we considered whether $\partial^{15}N$ and $\partial^{13}C$ values from animals inhibiting in the cold current ocean regions of Japan may be higher and lower than those in the warm current region, respectively. The marked differences in $\partial^{13}C$ between samples from the northern and southern region (Table 1) cannot be fully explained by the effect of latitude (*8*), as the expected difference in $\partial^{13}C$ calculated from the difference in latitude between Abashiri and Nago (18°) is only 0.27‰. Unfortunately, little information is available regarding geographical variations in $\partial^{13}C$ and $\partial^{15}N$ in marine biota around Japan. Takai et al. (*6*) reported lower $\partial^{13}C$ values in squid samples from the northwest of the Sea of Japan. Similarly, $\partial^{13}C$ in Baird's beaked whales hunted in this area was lower than in whales from other areas (see Figure S1). Tanaka et al. (*7*) suggested lower $\partial^{13}C$ and $\partial^{15}N$ values in the Kuroshio extension and Kuroshio-Oyashio transition zones. To precisely estimate the trophic position of toothed whales, dolphins, and porpoise around Japan and compare with the trophic level from different areas, measurements of $\partial^{13}C$ and $\partial^{15}N$ in primary producers (the base of the food web) around Japan are necessary (*11*).

On the other hand, T-Hg concentrations in the samples from southern Japan were apparently higher than those from northern Japan (Figure 2). As suggested previously (*12, 17*),